Early Cambrian organophosphatic brachiopods from the Xinji Formation, Shuiyu section, North China

Bing Pan [a, b, c], Christian B. Skovsted [c, d], Glenn A. Brock [e], Timothy P. Topper [c, d], Lars E. Holmer [d, f], Luoyang Li [c, d], Guoxiang Li [a, *]

[a] *State Key Laboratory of Palaeobiology and Stratigraphy*, *Nanjing Institute of Geology and Palaeontology and Center for Excellence in Life and Paleoenvironment, Chinese Academy of Sciences*, *Nanjing 210008*, *China*

[b] *University of Science and Technology of China, Hefei 230026, China*

[c] *Department of Palaeobiology*, *Swedish Museum of Natural History*, *Box 50007*, *SE-104 05 Stockholm*, *Sweden*

[d] *Shaanxi Key Laboratory of Early Life and Environments*, *Department of Geology*, *State Key Laboratory of Continental Dynamics*, *Northwest University*, *Xi'an 710069*, *China*

[e] *Department of Biological Sciences and Marine Research Centre*, *Macquarie University*, *Sydney*, *NSW 2109*, *Australia*

[f] Institute of Earth Sciences, Palaeobiology, Uppsala University, SE-752 36, Uppsala, Sweden

[*] Corresponding author

Abstract

Abundant and diverse small shelly fossils have been reported from rocks of Cambrian Series 2 in North China, but the co-occurring brachiopods are still poorly known. Herein, we describe

seven genera, five species and three undetermined species of brachiopods including one new genus and one new species from the Cambrian Xinji Formation at Shuiyu section, located on the southern margin of North China Platform. The brachiopod assemblage comprises one mickwitziid (stem-group brachiopod), *Paramickwitzia boreussinaensis* n. gen, n. sp., a paterinide, *Askepasma toddense* Laurie, 1986, an acrotretoid, *Eohadrotreta* cf. *zhenbaensis* Li and Holmer, 2004, a botsfordiid, *Schizopholis yorkensis* (Holmer and Ushatinskaya, 2001) and three linguloids, *Spinobolus* sp., *Eodicellomus* cf. *elkaniiformis* Holmer and Ushatinskaya, 2001 and *Eoobolus* sp. This brachiopod assemblage suggests a late Stage 3 to early Stage 4 age for the Xinji Formation and reveals a remarkably strong connection with coeval faunas from east Gondwana, particularly the Hawker Group in South Australia. The high degree of similarity (even at species level) further supports small shelly fossil data that indicate a close palaeogeographic position between the North China Platform and Australian East Gondwana during the early Cambrian.

1. Introduction

Cambrian Series 2 strata have a wide distribution along the western, southern and eastern margin of North China Platform (NCP) (Zhang and Zhu, 1979; Zhang et al., 1979; Liu, 1986). In the past several decades, many metazoan skeletal fossils have been published from the Xinji and Houjiashan formations which crop out extensively along the western and southern margin of the NCP (He et al., 1984; Yu, 1984; He and Pei, 1985; Xiao and Zhou, 1984; Zhou and Xiao, 1984; Li et al., 2014; Pan et al., 2015, 2017, 2018a, 2018b; Li et al., 2016, 2017; Skovsted et

al., 2016; Yun et al., 2016). However, to date only one brachiopod taxon, *Kutorgina sinensis* Rong in Lu 1979, has been illustrated but not described (Lu, 1979). Other brachiopod taxa have been briefly mentioned, but no detailed taxonomic assessment has ever been published (He et al., 1984; Xiao and Zhou, 1984; Yu et al., 1984; Zhou and Xiao, 1984; Liu, 1986). In addition, the possible stem group brachiopod, *Apistoconcha* cf. *apheles* has been reported from the Xinji Formation at Shangwan section, Shaanxi Province (Li et al., 2014). Broadly coeval lower Cambrian organophosphatic brachiopod assemblages have been described from other continents, including Australia (Kruse, 1990; Brock and Cooper, 1993, Ushatinskaya and Holmer, 2001; Topper et al., 2013; Betts et al., 2016), Antarctica (Holmer, 1996; Claybourn, 2017), South China (Li and Holmer, 2004; Zhang et al., 2015; Z.F. Zhang et al., 2016; Z.L. Zhang et al., 2016; Zhang et al., 2018a; 2018b), Siberia (Kouchinsky et al., 2015; Ushatinskaya and Korovnikov, 2014, 2016; Skovsted et al., 2015), Greenland (Skovsted and Holmer, 2003, 2005; Skovsted et al., 2010), Canada (Landing et al., 2002; Balthasar, 2004; Skovsted et al., 2017) and the United States of America (Rowell, 1977; Skovsted, 2006b; Skovsted and Peel, 2010; Butler, 2015). Here, we report an abundant brachiopod fauna from the Xinji Formation at Shuiyu section, Ruicheng County, Shanxi Province that show very close similarity with faunas described from Australian East Gondwana. New systematic descriptions of brachiopods from North China make an important contribution to Cambrian diversity amongst metazoan skeletal fossils in North China but also extend the known global distribution and refine evolutionary relationships and stratigraphic correlation of linguliform brachiopods during Cambrian Epoch 2.

2. Geological background

2.1 Locality and lithostratigraphy

All brachiopods were recovered from a 39.8 m succession of the Xinji Formation cropping out in Ruicheng County, Shanxi Province (Fig. 1A). The Xinji Formation at this locality represents the lowermost Cambrian strata and comprises a package of siliciclastic rocks intercalated with carbonates, which crops out extensively along the southwestern to southern margin of the North China Platform (Liu et al., 1991; Liu et al., 1994). In the Shuiyu section, the Xinji Formation disconformably overlies Precambrian strata; either the Luoquan Formation (predominantly diamictites), or Longjiayuan Formation (Palaeoproterozoic or Mesoproterozoic, grey dolostones; Fig. 1B). The Xinji Formation at the Shuiyu section can be subdivided into two parts: the lower part (7 m) is dominated by grey-black phosphatic conglomerates, purple-red shale and phosphatic sandstone; the upper part (32.8 m) consists of red quartz sandstone intercalated with argillaceous dolostone (Bureau of Geology and Mineral Resources of Shanxi Province, 1989). The brachiopod *Kutorgina sinensis* Rong in Lu 1979 was reported from the lower part of this section (Lu, 1979, pl. V, figs. 9–11). The basal 10.7 m of exposed section was sampled for shelly fossils since the top of the section is covered by alluvium and/or vegetation. There are abundant trace fossils in the lowermost rocks which belongs to a typical *Cruziana* ichnofacies (Miao and Zhu, 2014), indicating a subtidal environment for the basal Xinji Formation at Shuiyu section. The conformably overlying phosphatic quartz siltstone (1.2–4.2

m above the base) yields abundant brachiopods in the matrix (Fig. 1B). The brachiopods described herein were all retrieved from nodules with relatively more calcium carbonate within a strongly weathered bed of phosphatic quartz siltstone which occurs 3.4–3.8 m above the base of the Xinji Formation (Fig. 1B). It was not possible to obtain brachiopod specimens from the surrounding matrix at other layers (normally without calcium carbonate) by the processes of acetic acid leaching. Attempts at collecting specimens from the sandstone by other methods only resulted in fragmentary and generally undiagnostic specimens.

2.2. Biostratigraphy

No trilobites are known from the Xinji Formation at the Shuiyu section. However, the lower Cambrian Xinji Formation crops out widely along the southern and southwestern margin of North China Platform and other sections have yielded a small assemblage of trilobites including *Estaingia* (*Bergeroniellus*) *lonanensis* Hsiang in Lu et al., 1965 (Luonan County), *Estaingia (Hsuaspis) houchiuensis* Chang in Hsiang, 1963 (Luonan County), and *Redlichia* cf. *R. nanjiangensis* Zhang and Lin in Lee, 1978 (Queshan County) (Zhang and Zhu, 1979; Zhang et al., 1979; Miao, 2014). This trilobite assemblage has been correlated with the *Drepanuloides* Biozone of the middle Tsanglangpuan stage (Cambrian Stage 4) on the Yangtze Platform (Zhang and Zhu, 1979; Zhang et al., 1979; He et al., 1984; He and Pei, 1985; Miao, 2014). Miao (2014) correlated this trilobite assemblage with the *Pararaia janeae* trilobite Zone (Stage 4) assemblage of South Australia.

According to Yuan et al. (2011), the earliest occurrence of of *Redlichia* known from South China is *Redlichia* (*R.*) *premigena* Lin and Yin in Zhang *et al.* 1980 (Zhang *et al*. 1980, p. 125, pl. 19, figs 3–5) within the *Paokannia-Szechuanolenus* Zone and *Ushbaspis* Zone of the middle Tsanglangpuan (Canglangpuan) (Stage 4). But, the FAD of *Redlichia* (*Redlichia* sp.) in South Australia is from the *Pararaia bunyerooensis* Zone which is correlated with the *Yunnanocephalus* Assemblage subzone of the upper Chiungchussuan (Qiongzhusian) (Stage 3) of South China (Paterson and Brock, 2008; Topper et al., 2009; Betts et al., 2018). In South Australia, *Estaingia* is known from the *Pararaia janeae* Zone of Stage 4 (Oraparinna shale in Bengtson et al., 1990; Emu Bay Shale in Paterson et al., 2008; Betts et al., 2018). However, the first occurrence of *Estaingia* in South China is in the lower part of Shuijingtuo Formation of upper Stage 3 (Zhang et al., 1957; Li and Holmer, 2004; Dai and Zhang et al., 2012; Yang et al., 2015). Z.F. Zhang et al. (2016) reinterpreted the middle–upper *Tsunyidiscus*-bearing Shuijingtuo Formation in Hubei Province as possibly being Series 2 Stage 4 based on brachiopods correlation which means *Estaingia* also has an FAD in Stage 4 in South China. As such, the FADs of *Estaingia* and *Redlichia* in South China and South Australia are reversed. However, lateral diachronism and section loss (disconformable base) in the Xinji Formation across North China and within the Hawker Group in South Australia (Betts et al., 2018) may account for this regional biostratigraphic range reversal and likely truncation of the biostratigraphic ranges of these taxa so that the FAD of both *Estaingia* and *Redlichia* may still potentially occur at levels in upper Stage 3 then range into lower Stage 4. Since the global boundary for the base of Cambrian Stage 4 has not been formally defined the biostratigraphic

126 ranges of numerous taxa (including trilobites) are difficult to constrain – impeding global
127 correlation around this boundary.

128 The Xinji Formation has yielded abundant and diverse shelly fossils, such as hyoliths (He
129 et al., 1984; Pan et al., 2015; Skovsted et al., 2016), molluscs (He and Pei, 1985; Feng et al.,
130 1994; Li et al., 2017), tommotiids (Pan et al., 2018a), *Microdictyon* (Pan et al., 2018b) etc. from
131 various localities (Luonan, Yexian, Fangcheng and Longxian counties) usually co-occurring
132 with the trilobite assemblage mentioned above (Li et al., 2014; Li et al., 2016; Yun et al., 2016
133 and the references therein). Many of these shelly fossils, such as tommotiids (Pan et al., 2018a),
134 hyoliths (Skovsted et al., 2016; Pan et al., 2017), and other taxa (He and Pei, 1985; Feng et al.,
135 1994; Li et al., 2014; Li et al., 2016; Yun et al., 2017; Pan et al., 2018b) have been documented
136 from the *Dailyatia odyssei* Zone (Cambrian lower Stage 3 to lower Stage 4) in South Australia
137 (Bengtson et al., 1990; Gravestock et al., 2001; Topper et al., 2009; Betts et al., 2016, 2017;
138 2018). In conjunction with trilobite occurrences, the shared species of shelly fossils indicates
139 the Xinji Formation correlates to a Cambrian Series 2, upper Stage 3 to lower Stage 4. The
140 assemblage of brachiopods described herein also has a very strong Austral signal and further
141 strengthens this age assessment (see discussion of biostratigraphic significance).
142
143 **3. Material and methods**
144 All specimens were retrieved from samples of calcareous nodules between 3.4–3.8 m above
145 the base of the Xinji Formation at Shuiyu section, Shanxi Province. Specimens are more or less
146 fragmentary and many are encrusted with adhering quartz grains. All samples were treated in

6% acetic acid. Selected specimens were placed on pin-type stubs, gold coated and photographed using the Scanning Electron Microscopy facility at the Nanjing Institute of Geology and Palaeontology, Chinese Academy of Sciences (NIGPAS) (LEO 1530VP) and the Swedish Museum of Natural History (NRM) (HITACHI S-4300). All illustrated specimens are housed and catalogued in the storage facilities at NIGPAS.

4. Systematic paleontology

Terminology. The morphological terms follow the treatise of brachiopod (**). In the descriptions below we follow the suggestion by (see Zhang et al., 2018a, b for a full discussion) that the term 'metamorphic shell' as present on most planktotrophic Early Palaeozoic organophosphatic brachiopods should be replaced by 'metamorphic shell'. Zhang et al. (2018a, b) noted that the so-called "metamorphic shell" includes evidence of larval setae as evidenced by the pairs of setal sacs (see, e.g. Fig. 2B below) that are shed during metamorphosis and change from planktotrophy to sedentary juveniles.

Phylum Brachiopoda Duméril, 1806

Class Paterinata Williams, Carlson, Brunton, Holmer, and Popov, 1996

Order Paterinida Rowell, 1965 Superfamily Paterinoidea Schuchert, 1893

Family uncertain

Genus *Askepasma* Laurie, 1986

Type species. *Askepasma toddense* Laurie, 1986; *Micrina etheridgei* Zone (Cambrian, Stage 3), Todd River Dolostone, Northern Territory, Australia.

Diagnosis. See Laurie (1986, pp. 449) and Topper et al. (2013, pp. 98).

Remarks. Askepasma Laurie, 1986 and the type species, *A. toddense* Laurie, 1986, was erected by Laurie (1986) to accommodate paterinids from the lower Cambrian (Stage 3) Todd River Dolostone, Northern Territory, Australia that lacked a homeodeltidium. Subsequently, more abundant and better preserved specimens of *A. toddense* were reported from South Australia (Ushatinskaya and Holmer, 2001; Jago et al., 2006; Topper et al., 2013; Betts et al., 2016). Topper et al. (2013) also established a new species, *Askepasma saproconcha*, based on specimens from older strata in the Arrowie Basin. The first occurrence of *A. toddense* is mutually exclusive with the LAD of the older *A. saproconcha* suggesting a likely ancestor-descendent lineage for these species. *Askepasma transversalis* Peng, Zhao, Qin, Yan, and Ma, 2010 was erected by Peng et al. (2010) from the lower Cambrian Banglang Formation (Stage 4) in South China, though the generic affinity of this taxon is unclear (Topper et al., 2013) since many of the key generic character traits are not demonstrated in *A. transversalis*. The new discovery of conspecific *Askepasma toddense* from North China is thus the first secure report of *Askepasma* outside of Australia and provides a very strong biogeographic signal between the brachiopod faunas of North China and South Australia in the early Cambrian.

Askepasma toddense Laurie, 1986

(Fig. 2)

1986 *Askepasma toddense* – Laurie, p. 449, figs. 5G, 11A–O.

1998 ?*Aldanotreta* sp. – Williams et al., p. 222.

1998 *Paterina*? sp. – Williams et al., pl. 1, fig. 1, pl. 5, figs. 6–8.

1998 *Askepasma toddense* – Williams et al., pl. 3, figs. 6–7, pl. 4, figs. 1–3, pl. 8, figs. 1–8, pl. 10, fig. 9, pl. 11, fig. 11.

2001 *Askepasma*? sp. – Ushatinskaya and Holmer, p. 122, pl. 15, figs. 1–10, pl. 16, figs. 1–9.

2006 *Askepasma* sp. B – Jago et al., p. 414, fig. 4C, D.

2009 *Askepasma* – Balthasar et al., p. 1144, figs. 1C, F, H–J, 2E.

2013 *Askepasma toddense* – Topper et al., p. 98, figs. 2, 3.

2016 *Askepasma toddense* – Betts et al., p. 194, fig. 16A–H.

Material. 32 dorsal valves and 25 ventral valves from 3.4–3.8 m above the base of the Xinji Formation at Shuiyu section in Ruicheng County (Fig. 1).

Description. Shell ventribiconvex, subquadrate in outline (maximum width 1.84 mm, maximum length 1.81 mm of complete valves) with maximum width approximately mid-length. Straight hinge line. Ventral valve moderately to strongly convex (Fig. 2A, B, G and H). Ventral interarea high, flattened apsacline to catacline with open and wide delthyrium (Fig. 2F–H); pedicle callist changes from depressed to protruding beneath the apex through ontogeny (Fig. 2F_1 and F_2). Dorsal valve flattened to weakly convex, usually with a weakly expressed central

sulcus and two flattened and broad lateral slopes ranging anterolaterally from the apex to the margin (Fig. 2A, A_1 and B). Dorsal interarea well-defined, low and varying from anacline to hypercline (Fig. 2A–C and E); notothyrium broad, closed by a strongly arched, subtriangular homeochilidium (Fig. 2E). Ventral metamorphic shell (maximum width 680 μm), subrounded in outline with several (up to 10 7) clearly expressed, straight radial ribs (Fig. 2G). Dorsal metamorphic shell rounded and protruding (maximum width 400 μm) usually with 2 pairs of broad setal lobes (70–90 μm in width and 150–180 μm in length) as well as a central bulbous protegulum (about 120 μm across) (Fig. 2B).

External ornament of the post metamorphic shell consists of well developed, irregularly spaced, concentric growth lamellae (sometimes cut by short nick points, Fig. $2H_2$ and H_3) with a micro-ornament of fine reticulation (5 μm width) separating compressed, close-packed, polygonal pits (width ranging from 3 to 13 μm; long axes approximately parallel to the concentric lamellae (Fig. $2H_1$). The irregular, shallow polygonal pits on the metamorphic shell are less compressed than on the post metamorphic shell (Fig. $2B_1$). The inner surface of some dorsal valves displays a series of radiating ridges (width ca. 30 μm), diverging anteriorly (Fig. 2D).

Remarks. The specimens of *Askepasma toddense* described herein are very similar to those described from the Northern Territory (Laurie, 1986, figs 5G; 11A–O) and South Australia (Topper et al., 2013, figs. 2, 3). The only slight difference is that the ridges on the inner surface are usually absent in the specimens from North China which may be a preservational artefact. The metamorphic shells in the material from North China are identical morphology and size

range, with those from the Australian material, but the 2 pairs of bulbous lobes, representing setal sacs and the central node representing the protegulum are better preserved and more prominent in the present material (Fig. 2B$_1$). The main diagnostic difference between *A. toddense* and *A. transversalis* (South China) is the prominent pedicle beak and lack of reticulate external micro-ornament in the latter (Peng et al., 2010; Topper et al., 2013). However, the preservational differences between the 3-dimensional specimens of *A. toddense* usually recovered from shallow water carbonate (Laurie, 1986; Topper et al., 2013; herein) and the crack out specimens of *A. transversalis* preserved in shale from deep water, shelf to slope environments (Peng et al., 2010) complicates the detailed comparison. *Askepasma saproconcha* differs from the other two species by its well-developed, pronounced chevron-shaped fold in the dorsal valve and deep sulcus in the ventral valve, and less strongly mineralized shell with large void spaces of organic material forming a distinctive shell structure (Topper et al., 2013). The presence of *A. toddense* in both North China and South Australia provides additional support for a close connection of these two terranes in the early Cambrian.

Class Lingulata Gorjansky and Popov, 1985

Order Acrotretida Kuhn, 1949

Superfamily Acrotretoidea Schuchert, 1893

Family Acrotretidae Schuchert, 1893

Genus *Eohadrotreta* Li and Holmer, 2004

Type species. Eohadrotreta zhenbaensis Li and Holmer, 2004, Qiongzhusian (Cambrian, Stage 3), Shuijingtuo Formation in southern Shaanxi Province, South China.

Diagnosis. See Li and Holmer (2004, p. 204).

Remarks. *Eohadrotreta* was erected by Li and Holmer (2004) based on specimens from the lower part of the Shuijingtuo Formation in southern Shaanxi Province. Recently, *Eohadrotreta* was also reported from the Shuijingtuo Formation in Fangxian County (Yang et al., 2015) and the Three Gorges area (Z.F. Zhang et al., 2016) of western Hubei Province, the Parahio Formation (Stage 4) of the Tethyan Himalaya (Popov et al., 2015) and the *Dailyatia odyssei* Zone of South Australia (Betts et al., 2017), which indicate potential links among these contemporaneous brachiopod faunas.

Eohadrotreta cf. *zhenbaensis* Li and Holmer, 2004

(Fig. 3)

2004 *Eohadrotreta zhenbaensis* – Li and Holmer, p. 206, figs. 11–13.

2007 *Eohadrotreta zhenbaensis* – Holmer and Popov, p. 2560, figs. 1693, 1694.

2015 *Eohadrotreta zhenbaensis* – Yang et al., p. 1552, fig. 9E, F.

2016 *Eohadrotreta zhenbaensis* – Z.F. Zhang et al., p. 338, figs. 4, 5.

2016 *Eohadrotreta zhenbaensis* – Z.L. Zhang et al., p. 459, figs. 2–5.

? 2017 *Eohadrotreta* sp. cf. *E. zhenbaensis* – Betts et al., p. 269, fig. 15A–O.

2018a *Eohadrotreta zhenbaensis* – Zhang et al., p. 7, figs. 1, 2b–h, 3.

2018b *Eohadrotreta zhenbaensis* – Zhang et al., p. 4, figs. 3–6.

Material. 47 dorsal valves, 65 ventral valves from 3.4–3.8 m above the base of the Xinji Formation at Shuiyu section in Ruicheng County (Fig. 1).

Description. Shell ventribiconvex, subcircular to transversely ovoid in commissural outline (Fig. 3A and E); on average 87% as wide as long (n=17); maximum width near mid valve. Ventral valve is low, conical to gently convex with somewhat straight posterior margin; ventral pseudointerarea apsacline to procline with a shallow intertrough bisected by a fine undulating furrow (Fig. 3A_1–A_2). Pedicle foramen oval to elongated oval (average width 56 μm; average length 86 μm), not enclosed within the metamorphic shell (Fig. 3A_2, C and C_1); the foramen cuts across the post larval growth lines for the posterior 2/3 of its length (Fig. 3C and C_1). The sub circular ventral metamorphic shell (average diameter 175 μm) bears a slightly convex apex covered by uniform flat-bottomed hemispherical pits (diameter ca. 1 μm) (Fig. 3A, A_1, C and C_2), vanishing towards the margin of the metamorphic shell. Post-metamorphic shell ornamented with concentric fila usually interrupted by fold or drape-like nick points (Fig. 3A, C, D and D_1). Ventral interior with weakly expressed apical process covered by epithelial cell moulds (cell size, 10–20 μm) without apical pit on either side (Fig. 3B–B_2). The posterolateral muscle scars are poorly preserved (Fig. 3B and B_1). The intertrough is quite depressed inward (Fig. 3B_1).

293 Dorsal valve laterally ovoid in outline, moderately convex in lateral profile with maximum
294 width near the posterior 2/5 of shell length, on average 86% as wide as long (n=17).
295 Metamorphic shell sub circular and ornamented with uniform circular pits (1 μm in diameter)
296 lacking clear imprints of setal sacs. Post-metamorphic shell covered by moderately coarse
297 concentric growth lines (Fig. 3F). Narrow dorsal pseudointerarea orthocline bisected medially
298 by short subtriangular median groove (Fig. 3E and G). Propareas extend laterally with several
299 transverse wrinkles (Fig. 3G1). The strongly developed median buttress narrows anteriorly and
300 does not extend beyond the posterior 1/4 of valve length. Median ridge is weakly expressed,
301 rarely with a pair of inconspicuous submedian ridges (Fig. 3E and E1). Dorsal cardinal muscle
302 scars widely separated, preserved as prominent exfoliated areas, extending anterolaterally from
303 the lateral edge of the median groove, reaching ca 30% of the valve length (Fig. 3E, H and G).
304 Epithelial cell imprints (cell size, 14–25 μm) preserved on the inner surface of one specimen
305 (Fig. H1).
306 *Remarks*: The morphology of *Eohadrotreta* cf. *zhenbaensis* from North China is similar to *E.*
307 *zhenbaensis* reported from South China (Li and Holmer, 2004; Yang et al., 2015; Z. F. Zhang
308 et al., 2016; Z. L. Zhang et al., 2016, 2017) in general outline, apsacline to procline ventral
309 valve pseudointerarea, weakly expressed apical process without apical pits, narrow orthocline
310 dorsal pseudointerarea, strong dorsal median buttress, diverging dorsal submedian ridges and
311 metamorphic shell with pitted ornament not enclosing the oval pedicle foramen. However, the
312 specimens from North China differ in some characters, such as weaker median and submedian
313 dorsal ridges (lacking in many specimens) and the shallow ventral intertrough with a central

314 furrow. In South China, *E. zhenbaensis* often occur together with the morphologically similar
315 *Eohadrotreta*? *zhujiahensis* Li and Holmer, 2004 (Li and Holmer, 2004; Z.F. Zhang et al., 2016;
316 Zhang et al., 2018b). However, as discussed by Zhang et al. (2018b), *Eohadrotreta*?
317 *zhujiahensis* has a distinct post-metamorphic shell growth pattern with delayed enclosure of the
318 pedicle foramen and decreased length of the ventral intertrough, which is very different from
319 the situation in *Eohadrotreta* cf. *zhenbaensis* from North China. *Eohadrotreta haydeni* from the
320 Parahio Formation (Stage 4 and 5) in the Himalaya differs from the material from North China
321 by its poorly developed pseudointerarea and dorsal median septum as well as a very poorly
322 defined median buttress and short dorsal cardinal muscle scars (Popov et al., 2015). In most
323 aspects, except the presence of shallow apical pits, *Eohadrotreta* sp. cf. *E. zhenbaensis* from
324 South Australia (Betts et al., 2017, fig. 15A–O) is quite similar to the North China specimens.
325 However, the apical process and apical pits are very variable in descriptions of *Eohadrotreta*
326 by different authors (Li and Holmer, 2004; Holmer and Popov, 2007; Popov et al., 2015; Z.F.
327 Zhang et al., 2016; Z.L. Zhang et al., 2016) and it is possible that the presence of apical process
328 and apical pits in *Eohadrotreta* is related to ontogeny and preservation and not a suitable
329 characteristic for species determination. Thus, further work on well preserved adult specimens
330 will be required to resolve the taxonomy of this group of acrotretoids.
331
332 Order Lingulida Waagen, 1885
333 Family Obolidae King, 1846
334 Subfamily Obolinae King, 1846

335

336 Genus *Spinobolus* Zhang and Holmer, 2016

337

338 *Type species*. *Spinobolus popovi* Zhang and Holmer, 2016, Tsanglangpuan (Cambrian, Stage 4)

339 Shuijingtuo Formation Three Gorges area, Hubei Province, South China.

340 *Diagnosis*. See Z.F. Zhang et al., 2016 and Zhang, 2018 (emended).

341 *Remarks*. *Spinobolus* was established by Z.F. Zhang et al. (2016) based on specimens from the

342 Shuijingtuo Formation in the Three Gorges area, Hubei Province, South China, which lack

343 pitted metamorphic shell ornamentation and with distinct prone, spine-like pustules along the

344 marginal edge of the growth lines on the post-metamorphic shell. This ornamentation is clearly

345 distinguished from the widespread coeval genus *Eoobolus*. Recently, Zhang (2018, fig. 8.29A,

346 B) illustrated pitted ornamentation (diagnostic character trait of the family Eoobolidae) on the

347 metamorphic shell of *Spinobolus*, which makes the systematic position of the genus problematic

348 and Zhang (2018) considered reassigning *Spinobolus* to the Eoobolidae. However, current

349 evidence is inconclusive and we follow Zhang et al. (2018) in retaining the original assignment

350 of *Spinobolus* to the Obolidae King, 1846 originally proposed by Z.F Zhang et al. (2016).

351 *Spinobolus* was previously thought to be endemic to South China (Z.F. Zhang et al., 2016;

352 Zhang, 2018), but its distribution can now be extended to North China.

353

354 *Spinobolus* sp.

355 (Fig. 4)

356

357 *Material*. Two dorsal valves from 3.4–3.8 m above the base of the Xinji Formation at Shuiyu
358 section in Ruicheng County (Fig. 1).

359 *Description*. The shells are thin, slightly convex and oval in outline with a maximum width of
360 1.44 mm and length of 1.55 mm. The post metamorphic shell is ornamented by concentric
361 lamellae bearing prone obtuse pustules (ca. 10 μm in diameter). The metamorphic shell is
362 smooth (Fig. 4A). Dorsal pseudointerarea orthocline and low, slightly raised above the valve
363 floor and divided by a broad, shallow median groove forming an angle of ca. 80° (Fig. 4A$_3$).
364 Posterolateral muscle scars of the dorsal valve interior are not well. Median ridge well
365 developed, anteriorly widening and extending almost to the anterior margin of the valve (Fig.
366 4A$_3$). Weak *vascula lateralia* occur along the posterolateral margins (Fig. 4A$_4$).

367 *Remarks*. Despite the limited number of specimens and relatively poor preservation of the
368 specimens from North China, the two recovered valves show distinct surface ornamentation
369 and some internal structures (broad median groove, posterolateral muscle scars, prominent
370 median ridge and weak *vascula lateralia*) that indicate affinities with the genus *Spinobolus* from
371 South China. The concentric lines of prone obtuse pustules are arranged like in *Spinobolus* with
372 older spines superimposed on the newer, an arrangement which is different from the ornament
373 of coeval *Eoobolus* which has all pustules distributed on the same surface. The pustules of the
374 North China specimens of *Spinobolus* (Fig. A$_2$) differ slightly from *Spinobolus popovi* from
375 South China (Z.F. Zhang et al., fig. 7D) in the more rounded shape of the spinose extensions.
376 However, the lack of specimens from North China makes comparison of the pustule shape

377 difficult and any differences could be either preservational or interspecific variation. Thus, we
378 assign these two valves to open specific nomenclature, *Spinobolus* sp. and hope that retrieval
379 of more specimens may help resolve the taxonomy of this taxon. The lack of a pitted
380 metamorphic shell ornament could also be a preservational artifact as illustrated in specimens
381 described by Z.F. Zhang et al. (2016, fig. 7).
382
383 Genus *Eodicellomus* Holmer and Ushatinskaya, 2001
384
385 *Type species. Eodicellomus elkaniiformis* Holmer and Ushatinskaya, 2001; *Dailyatia odyssei*
386 Zone (Cambrian Stage 3), Parara Limestone, Yorke Peninsula, South Australia.
387 *Diagnosis*. See Holmer and Ushatinskaya, 2001, p. 125.
388 *Remarks*. *Eodicellomus* was established by Holmer and Ushatinskaya (2001) based on the
389 specimens from the Parara Limestone of Yorke Peninsula and the Ajax Limestone and
390 Mernmerna Formation of the Flinders Ranges, South Australia. *Eodicellomus* is distinguished
391 by thick biconvex shells with visceral platforms in both valves, a broadly triangular ventral
392 pedicle groove, deep and gently curved ventral *vascula lateralia* and the longer and deeper
393 dorsal *vascula media*. The specimens from North China illustrated herein match these
394 characters in most respects. However, the metamorphic shell of the North China specimens
395 exhibits a distinct pitted micro ornament which has not been reported in specimens from South
396 Australia. This difference is probably related to variation in preservation of surface sculpture in
397 specimens from the two regions.. This is the first report of *Eodicellomus* outside Australia which

provide further evidence of the strong biogeographic signal between the brachiopod faunas of North China and South Australia in the early Cambrian.

Eodicellomus cf. *elkaniiformis* Holmer and Ushatinskaya, 2001

(Figs. 5, 6)

Material. 56 dorsal valves and 87 ventral valves from 3.4–3.8 m above the base of the Xinji Formation at Shuiyu section in Ruicheng County (Fig. 1).

Description. Ventral valves subrounded in outline with length (0.56–1.8mm) about 81-92% of width (0.68–2.2 mm) in complete specimens. Angle formed by posterolateral margins is large (ca. 150°), but the apex itself is sharper (110°) (Fig. 5B_1, B_2, C_2 and F–H). Posterior part of ventral valve is strongly convex (Fig. 5A–C). Ventral metamorphic shell is rounded (165–220 μm) and protruding with a small convex notch at the open posterior margin (Fig. 5C_2 and D); orientation of metamorphic shell nearly vertical to the adult commissural plane (Fig. 5B and C). Well-developed triangular ventral pseudointerarea highly elevated above valve floor and significantly changes from nearly catacline (Fig. 5E and E_1) to orthocline (Fig. 5A_2, B_2 and H–J) during ontogeny. Pseudointerarea (0.3–3 mm in width, 0.13–1.1 mm in length) divided by a deep and wide pedicel groove (0.1–1.1 mm in width), forming an angle of about 50°–80°. Propareas wide and raised high above groove. Flexure lines prominent; areas between flexure lines and lateral margins narrow and inclined in relation to propareas (Fig. 5E and H–J). Large, elongated posterolateral muscle scars located beneath propareas (Fig. 5A_2 and H–J). Central

muscle scars straight and wide, extending from near anterior margin of pedicle groove (Fig. 5A$_2$, H and H$_1$).

All dorsal valves incomplete but appear thick shelled, convex and subrounded in outline. In the most complete specimen (Fig. 6B$_2$), length and width equals 1.72 mm and 1.63 mm respectively. Metamorphic shell rounded (200–230 μm in diameter) and protruding (Fig. 6B). Posterior margin extending posterolaterally in early ontogeny (Fig. 6F), becoming straight in mature shells (Fig. 6C). Dorsal pseudointerarea well developed, apsacline to orthocline; median groove triangular, deep and wide; propareas weakly developed without obvious boundary with pedicle groove; flexure lines prominent; area outside flexure lines of some specimens with growth layers well separated (Fig. 6A). Elongate, paired posterolateral muscles scars elevated above valve floor, situated on posterolateral slopes, extending from lateral margin of the median groove at an obtuse angle (ca. 110°) (Fig. 6A–C). The highly raised platform in front of the anterior margin of the median groove usually composed of two wide and long lateral lobes and one narrow central lobe, all of which may fuse to form an apical process in some specimens (Fig. 6C and C$_1$). Central muscle scars wide, robust, and extending anterolaterally from the margin of the platform towards the anterior margin of the valve (Fig. 6B$_2$, B$_3$, C and C$_1$). *Vascula lateralia* well developed, ranging from lateral side of the platform (Fig. 6C, C$_1$, E).

Metamorphic shell ornamented by numerous microscopic pits (ca. 1 μm in diameter) (Figs 5C$_1$ and 6D). Post-metamorphic shell covered by coarse and uneven concentric growth lines (Figs 5A–C, 6B$_1$ and E$_1$). The dorsal metamorphic shell has two pairs of lobes (Fig. 6E$_2$).

Remarks. Although, the specimens are not very well preserved and usually incomplete, they still quite similar to *Eodicellomus elkaniiformis* Holmer and Ushatinskaya, 2001 in many aspects, such as the subrounded outline, the strongly convex valves, the wide angle of the ventral posterior margin with a relatively sharp apex (compare Fig. 5H to Holmer and Ushatinskaya, 2001, pl. 19, figs 1a and 2), the wide triangular pedicle groove, the well developed muscles scars of both ventral and particularly dorsal valves (compare Figs. 6A–C toBetts et al., 2016, fig. 17L). However, the ventral valves from North China only have two straight central muscle scars (Figs. 5A_2 and H) instead of a ventral visceral platform (Holmer and Ushatinskaya, 2001, pl. 19, figs 1; Betts et al., 2016, 17I, K and M), and the muscles scars and visceral area in the dorsal valves from North China (Fig. 6) are less well developed than these from South Australia (Holmer and Ushatinskaya, 2001, pl. 19, figs. 9–11; Betts et al., 2016, 17L). Another distinct difference is that the metamorphic shell in the specimens from North China have microscopic pits (Figs 7C_1 and 8D) which is usually smaller (less than 2mm in diameter) compared to the South Australian specimens (more than 3mm in diameter). However, the ventral visceral platform is also missing in poorly preserved ventral valves from South Australia (GAB personal observation 2018). Consequently, these differences could be a consequence ofdifferential preservation in the two areas and herein we refer the specimens from North China to *Eodicellomus* cf. *elkaniiformis* Holmer and Ushatinskaya, 2001. More detailed study of the morphology and variability of *Eodicellomus* from South Australia will be required to resolve the remaining uncertainties.

Family Eoobolidae Holmer, Popov and Wrona, 1996

Genus *Eoobolus* Matthew, 1902

Eoobolus sp.

(Fig. 7)

Material. 39 dorsal valves, 54 ventral valves and 9 articulated shells from 3.4–3.8 m above the base of the Xinji Formation at Shuiyu section in Ruicheng County (Fig. 1).

Description. Shells elongately ovoid, ventribiconvex with ventral valves slightly larger than dorsal valves (Fig. 7B); length (0.6–3.9 mm) about 85% of width (0.7–4.3 mm).

Ventral valve evenly convex, elongately ovoid with a blunt apical angle (99°–115°) (Fig. 7A and C). Triangular ventral pseudointerarea orthocline, raised and bisected medially by a broad and deep pedicle groove; the surface of the pedicle groove is ornamented with transverse and longitudinal lines; the angle formed by the pedicle groove ranges from 35° to 51°. Lateral margins of the pseudointerarea are gently curved. Pseudointerarea is divided by strongly marked flexure lines and the propareas are narrow (Fig. 7A, A_1 and A_2). The tear drop-like ventral posterolateral muscle scars are large (ca. 0.5 mm) and elongate, extending anteriorly from the base of the propareas parallel to the direction of the margins of the pedicle groove (Fig. 7A and A_1). Impressions of paired pedicle nerves are preserved in some specimens (Fig. 7A).

Ventral valve visceral area is weakly preserved with one pair of arcuate *vascula lateralia* diverging proximally (Fig. 7A).

Dorsal valve is gently convex and ovoid to suboval in outline (Fig. 7G and G$_1$). Dorsal valve pseudointerarea slightly elevated above valve floor, with a broad median groove bearing an anterior projection (Fig. 7E$_3$). Flexure lines unclear. Posterolateral muscle scars tear drop-like in outline (ca. 0.85 mm) (Fig. 7E$_3$, F). Low and broad median tongue occupies almost the whole length of the valve with a pair of relatively wide submedian ridges diverging at mid length (Fig. 7E$_3$, F, F$_1$ and H). Paired *vascula lateralia* weakly expressed (Fig. 7F).

The subrounded ventral metamorphic shell (180–250 μm in diameter) is ornamented with microscopic pits (ca. 0.8 μm, Fig. 7C$_1$). Posterior part of ventral metamorphic shell slightly elevated longitudinally (Fig. 7C). Ornament of dorsal metamorphic shell poorly preserved but fine wrinkles parallel to posterior edge are present on some specimens (Fig. 7B$_1$). Postlarval ornament variable of both valves with fine concentric fila with nick points and sometimes fine radial lines (Fig. 7C$_2$, D$_1$, D$_2$, E$_2$), but numerus small tubercles are present on the growth lines in some parts of shells (Fig. 7E, E$_1$ and G). .

Remarks. *Eoobolus* sp. show typical characteristics of the genus, such as microscopic pits on the larval and post-metamorphic shell with concentric growth lines with short pustules, raised triangular pseudointerarea with deep pedicle groove, well developed ventral flexure lines and imprints of pedicle nerves. The post-metamorphic shell ornament of *Eoobolus* sp. is quite variable, from continuous growth lines to separated pustules (Fig. 7B–E), comparing well with the ornament of specimens illustrated from other areas (e.g., Li and Holmer, 2014, fig. 6C).

Currently, a number of species of *Eoobolus* has been erected based on phosphatized, 3-dimensional specimens and crack out specimens (Holmer et al., 1996; Holmer and Popov, 2000; Ushatinskaya and Korovnikov, 2014; Popov et al., 2015 and the references therein), but, the distinction of many of these species is still not clear. Consequently, it is hard to place the specimens from North China in any established species of *Eoobolus* and here we take a conservative approach and assign the specimens to *Eoobolus* sp. rather than adding to the proliferation a new species in this "catchall" genus.

A single eoobolid specimen was recovered with a much more acute apical angle (75°), subparallel pedicle groove margins and relatively wide propareas (Fig. 8) compared to the majority of specimens referred to *Eoobolus* sp. This specimen is somewhat comparable to material referred to *E. priscus* (Poulsen, 1932), with an almost global distribution in Cambrian Stage 4 strata (Skovsted & Holmer 2005). However, this single fragmentary specimen is difficult to identify with certainty and is left in open nomenclature.

Superfamily Acrotheloidea Walcott and Schuchert, in Walcott, 1908

Family Botsfordiidae Schindewolf, 1955

Genus *Schizopholis* Waagen, 1885

1885 *Schizopholis* Waagen (type species, *Schizopholis rugosa* Waagen,1885)

1885 *Discinolepis* Waagen (type species, *Discinolepis granulata* Waagen, 1885)

1986 *Karathele* Koneva (type species, *Karathele coronata* Koneva, 1986)

Type species. *Schizopholis rugosa* Waagen,1885, lower Cambrian, Khussak Formation (lower *Neobolus* beds), Salt Range, Pakistan.

Diagnosis. See Popov et al. (2015, p. 376).

Remarks. *Schizopholis* was established by Waagen (1885) based on the specimens from Khussak Formation (lower *Neobolus* beds), Salt Range, Pakistan. Popov et al. (2015) provided a detailed discussion about the relationship of *Schizopholis*, *Discinolepis* and *Karathele* and confirmed that the latter two genera represent junior synonyms of *Schizopholis*. *Schizopholis* has been reported from Himalaya, Kazakhstan, Australia and Antarctica (Waagen, 1885; Koneva, 1986; Kruse, 1990; Holmer et al., 1996; Ushatinskaya and Holmer, 2001; Jago et al., 2006; Percival and Kruse, 2014; Betts et al., 2016; 2017). Herein, the first occurrence of *Schizopholis* in the Xinji Formation extends its palaeogeographic distribution in the early Cambrian to North China and provide further indication that the brachiopod fauna of North China belongs to the low-latitude ‘east’ Gondwana region (Popov et al., 2015, p. 354–356).

Schizopholis yorkensis Holmer and Ushatinskaya, 2001

(Fig. 9)

2001 *Karathele yorkensis* – Ushatinskaya and Holmer, p. 128–129, pl. XXI, figs. 1–11.

2006 *Karathele yorkensis* – Jago et al., p. 415, fig. 4O, P.

2016 *Karathele yorkensis* – Betts et al., p. 195, fig. 17A–H.

2017 *Karathele yorkensis* – Claybourn, p. 16, fig. 6A–E.

Material. 1 dorsal valve, 22 ventral valves and 2 articulated shells from 3.4–3.8 m above the base of the Xinji Formation at Shuiyu section in Ruicheng County (Fig. 1).

Description. The recovered specimens are fragmentary, but the structures of the valves are well preserved. The shell is thin and subcircular in outline (width 0.7 to 2.1 mm, length 0.6 to 2.2 mm preserved), with maximum width near mid-length. Ventral valve gently convex with strongly elevated umbo (Fig. 9A–A_2). Ventral valve metamorphic shell is rounded, covered by numerous microscopic pits (2 to 3 μm in diameter) and has a high median tubercle and sometimes a relatively low arcuate ridge surrounding the tubercle (Fig. 9A_2 and B_1). The diameter of the metamorphic shell varies from 246 to 420 μm. Post-metamorphic shell ornamented by concentric growth lines and irregularly distributed pustules (ca. 5 μm in diameter) (Fig. 9B and B_1). Ventral pseudointerarea is always incomplete, apsacline to catacline (Fig. 9A–A_3 and C). Pedicle groove deep and triangular with the two lateral margins curving towards the centre but not convergent (Fig. 9A_3). Ventral propareas vestigial (Fig. 9C and E). Posterolateral muscles scars elongated (Fig. 9C). Dorsal valve weakly convex in the central part and flattened anteriorly and laterally, slightly smaller than the ventral valve (Fig. 9E). Dorsal metamorphic shell (250 to 390 μm in diameter) with pitted ornamentation and two strongly protruding, high tubercles (Fig. 9D_1 and E). Post-metamorphic shell covered by numerous pustules (Fig. 9D_1 and E). Dorsal pseudointerarea low, with poorly developed median groove

(propareas and flexure lines unknown) (Fig. 9D). Median ridge short and narrow but prominent (not reaching to mid-length of the valve) (Fig. 9D). Posterolateral muscles scars elongate (Fig. 9D).

Remarks. The specimens from North China are essentially identical to *Schizopholis yorkensis* (Holmer and Ushatinskaya, 2001) from South Australia (Ushatinskaya and Holmer, 2001; Jago et al., 2006; Betts et al., 2016) in the triangular delthyrial opening with lateral delthyrial margins converging while remaining separated by a wider margin than in *S. napuru* (Kruse, 1990). The only difference is the reported size of the metamorphic shell (150–160 μm in diameter) in the Australian specimens (Ushatinskaya and Holmer, 2001). However, new measurements of the illustrated metamorphic shells (Ushatinskaya and Holmer, 2001, pl. XXI, figs. 6a, 8b, 7b, 9) suggests their diameter ranges from 175 to 333 μm. Furthermore, the diameter of metamorphic shell in specimens from South Australia illustrated by Betts et al. (2016, fig. 17D, F, G) is 361 to 387 μm. These results overlap the diameter of the specimens from North China (246 to 420 μm). In addition to South Australia and North China, *S. yorkensis* has also been reported from Antarctica by Claybourn (2017), further strengthening the faunal links of North China with these areas.

Stem group Brachiopoda

Family Mickwitziidae Goryansky, 1969

Genus *Paramickwitzia* n. gen.

585

586 *Etymology*. *Para*, similar. Referring to the similarity to the genus *Mickwitzia* Schmidt, 1888.

587 *Type and only species*. *Paramickwitzia boreussinaensis* n. sp.

588 *Diagnosis*. Shell gently convex with sub-marginal apex in both valves. Ventral metamorphic
589 shell heart shaped, raised above posterior margin and with low apsacline, ventral
590 pseudointerarea. Dorsal metamorphic shell gently dome-shaped with two pairs of lobes around
591 the protegulum; dorsal pseudointerarea orthocline (may later change to catacline during
592 ontogeny). Pseudointerareas of both valves wide, with poorly defined pedicle groove. Both
593 valves with unevenly distributed open pores along posterior margin and between growth
594 increments on pseudointerarea, sometimes associated with tubular indentations of previously
595 formed shell layers (indicating shell penetrating setae on pseudointerareas). External ornament
596 of fine radial costellae and concentric ridges with rounded pustules formed at intersections.
597 Internal surfaces with hollow cone-shaped projections associated with tubules penetrating the
598 secondary but not the primary shell.

599 *Remarks*. The hollow cones on the internal surface of the shell and the corresponding tubules
600 penetrating through the shell clearly align *Paramickwitzia* to the problematic mickwitziids
601 *Mickwitzia* Schmidt, 1888, *Heliomedusa* Sun and Hou, 1987, *Setatella* Skovsted, Streng,
602 Knight and Holmer, 2010 and *Kerberellus* Devaere, Holmer and Clausen, 2015. The exact
603 function of mickwitziid tubules is uncertain although they are interpreted to have been occupied
604 by soft tissue (Holmer et al., 2008a; 2014; Butler et al., 2015). Similar tubules, sometimes with
605 exceptionally preserved setae (Butler et al., 2015; Kouchinsky and Bengtson, 2017), are also

present in the more basal stem group brachiopods (tannuoliniid tommotiids *Micrina* Laurie, 1986, *Oymurania* Kouchinsky et al., 2015 and *Tannuolina* Fonin and Smirnova, 1967; Holmer et al., 2008b; Skovsted et al., 2014), and have been used to indicate a position of mickwitziids in the stem group of the Brachiopoda (Skovsted and Holmer, 2003; Skovsted et al., 2014).

The marginal position of the ventral apex, the presence of a pseudointerarea in both valves and the presence of shell penetrating setae (open tubes) on the pseudointerarea of *Paramickwitzia* is strongly reminiscent of *Setatella*, known from Cambrian Stage 4 in North-East Greenland and southern Labrador (Skovsted and Holmer, 2003; Skovsted et al., 2010). However, internal cone-shaped projections around the shell perforations are not present in *Setatella* but is instead characteristic of *Mickwitzia* (Balthasar, 2004; Skovsted et al. 2009; Butler et al., 2015). This combination of characters demonstrates that the specimens from North China represent a new mickwitziid genus and suggest that *Paramickwitzia* may occupy an intermediate position between *Setatella* and *Mickwitzia* in the brachiopod stem group. Detailed comparison of *Paramickwitzia* to *Heliomedusa* from South China is precluded since the latter taxon is only known from specimens preserved in shale, but present knowledge indicates that it has a sub-central ventral apex and no ventral pseudointerarea (Chen et al., 2007; Zhang et al., 2009). Comparison to *Kerberellus* is even more problematic as this taxon is only known from internal moulds, but it differs from *Paramickwitzia* by having catacline interareas without shell penetrating tubes in both valves (Devaere et al., 2015). Herein, we temporarily assign *Paramickwitzia* to Mickwitziidae Goryansky, 1969, noting that the relationships between mickwitziid taxa are still uncertain and that the present taxonomic framework can only be

627 regarded as provisional. Indeed, the discovery of *Paramickwitzia* in North China, indicates that
628 the diversity of the mickwitziid group may be significantly higher than previously assumed and
629 that future research on this problematic group may reveal important clues regarding the early
630 evolution of the Brachiopoda.
631
632 *Paramickwitzia boreussinaensis* n. gen et sp.
633 (Figs. 10, 11)
634
635 *Etymology*. *Boreus*, north; *sina*, China. *Boreussinaensis* referring to the discovery of this species
636 in North China.
637 *Holotype*. NIGPAS168765, dorsal valve (Fig. 11B–B$_5$) from3.4–3.8 m above the base of the
638 Xinji Formation, Shuiyu section, Ruicheng County, Shanxi Province.
639 *Diagnosis.* Same as for genus.
640 *Material.* Two dorsal valves (incomplete), Two ventral valves (incomplete) and 26 shell
641 fragments from 3.4–3.8 m above the base of the Xinji Formation at Shuiyu section in Ruicheng
642 County (Fig. 1).
643 *Description*. Only fragmentary shells were recovered but at least four specimens preserve the
644 posterior margin (two ventral and two dorsal valves) and the shells appear to be gently biconvex
645 with sub-equal valves. Ventral and dorsal valves differentiated by different shape and growth
646 pattern of the metamorphic shell and different inclination of the pseudointerareas. The curved
647 outline of the posterior margin suggests both of the gently convex valves have a subcircular

outline. Apex of both valves situated near the posterior margin (Figs. 10A and B, 11A and B). Ventral apex marginal and raised above posterior margin; smooth heart-shaped metamorphic shell surrounded by fine growth lines, diameter 102 μm (Fig. 10A_2, A_9, A_{10}, B_2 and B_3). Dorsal apex lower with concave lateral slopes separated from the posterior margin by a low ridge and shallow furrow (Fig. 11B, B_2 and B_5). Dorsal metamorphic shell about 90 μm in diameter with 2 pairs of poorly preserved setal lobes (about 20 μm wide) and a possible central protegulum (Fig. 11A_2). Ventral pseudointerarea wide, gently apsacline with relatively deep but poorly defined pedicle groove and ill-defined flat propareas without flexure lines (Fig. 10A_3). Terrace-forming growth-lines continue unchanged across propareas and pedicle groove (Fig. 10A_3). Dorsal pseudointerarea is similar in morphology with a deep pedicle groove but is orthocline in aspect (Fig. 11B_1 and B_2). A single dorsal valve has faint radial lines on the propareas and in this specimen the direction of the growth of the pseudointerarea changes abruptly after 200 μm from orthocline to catacline, and the pedicle groove is not developed after this change (Fig. 11B_1–B_3). All valves ornamented with radial costellae and concentric ridges of about equal width (Figs. 10A and B, 11A, B and D). New costellae originate between previously formed costellae (Fig. 11D_1). Small rounded pustules are present at intersections between radial and concentric ornament (Fig. 11D). Average diameter of pustules 25 μm, but they increase in size away from the metamorphic shell. Inner surface exhibits characteristic cone-shaped internal projections surrounding circular shell perforations at apparently random intervals (Fig. 11C). Diameter of cones is ca. 35 μm on average with inner diameter of central perforation ca. 12 μm and cones are typically ca. 40 μm high. Central perforation of cones continue as vertical tubules

669 through the shell but does not penetrate outermost (primary) shell layer. Perforations often, but
670 not always, aligned with pustules formed at intersection of radial and concentric ornament.
671 Numerous small circular holes (ca. 10 μm in diameter) penetrate the shell along the posterior
672 margin and on the pseudointerarea of both valves (Figs. 10A, A_1, A_6 and B_1, 11B_1–B_4). In some
673 specimens, open perforations on pseudointerarea aligned with cylindrical depressions on
674 preceding shell increments (Figs. 10A_3, A_6, 11B_4).

675 *Remarks*. Although *Paramickwitzia boreussinaensis* n gen. et sp. is only represented in our
676 material by fragmentary specimens, the well preserved posterior margins of both ventral and
677 dorsal valves yields enough information to clearly delineate the new taxon. Even small shell
678 fragments are clearly distinct from any other brachiopod species in the material from North
679 China by the unique surface ornamentation of radial costellae and concentric ridges and by the
680 characteristic shell tubules with internal cone-shaped extensions. These characteristics, together
681 with the wide, simple pseudointerareas with poorly defined pedicle grooves in both valves
682 indicate that these shells are derived from a mickwitziid stem group brachiopod. The dorsal
683 metamorphic shell illustrated herein (Fig. 11A and A_2) is closely similar to that of *Mickwitzia*
684 described by Balthasar (2004, 2009) in the two pair lobes and the shape of the protegulum, but
685 their smaller size (90 μm in diameter compared to 180 μm in *Mickwitzia*) and the direction of
686 the lobes (Fig. 11 A_2 VS figs. 2 and 4I in Balthasar, 2004) are different. The heart shaped ventral
687 metamorphic shell raised above the posterior margin (102 μm in width) (Fig. 10 A_9, A_{10} and B_3)
688 is also somewhat similar to that of *Mickwitzia* where the metamorphic shell is convex and
689 semicircular (140 μm in diameter). However, there is no homeodeltidium posteriorly of the

690 metamorphic shell in either the dorsal or ventral valves from North China like in *Mickwitzia*
691 (Balthasar, 2004, fig. 4B–E and B–D). Furthermore, pseudointerareas,which are apparent in
692 both valves from North China (Figs 10, 11) have never been reported in *Mickwitzia* (Balthasar,
693 2004; Butler et al., 2015). Mickwitziids are best known from the palaeocontinents Baltica and
694 Laurentia (Skovsted and Holmer 2003; Balthasar, 2004; Skovsted et al., 2010; Butler et al. 2015
695 and references therein) but in Gondwana and associated terrains, mickwitziid brachiopods are
696 rare. Exceptions include *Heliomedusa* from the Chengjiang biota of South China (Chen et al.,
697 2007; Zhang et al., 2009), *Microschedia amphitrite* Geyer, 1994 from Morocco and *Mickwitzia*
698 sp. from South Australia (Skovsted et al., 2009). However, all of these taxa differ from
699 *Paramickwitzia boreussinaensis* by having a sub-central apex on at least one valve (ventral)
700 and lacking pseudointerareas. Instead, the strongest similarity of *Paramickwitzia*
701 *boreussinaensis* is to *Setatella significans* Skovsted, Streng, Knight and Holmer, 2010 from
702 Greenland and Labrador on the eastern margin of Laurentia. *Paramickwitzia boreussinaensis*
703 differs from *S. significans* by the sub-equal development and the presence of pedicle grooves
704 in of both valves. The dramatic change in growth angle seen in one dorsal valve of *P.*
705 *boreussinaensis* is difficult to interpret but may be a response to a disturbance of the shell during
706 ontogeny. More specimens will be needed to analyse the origin of this structure.

707 The tubules in the main part of the shells of *Paramickwitzia boreussinaensis* are closed
708 externally and are oriented perpendicular to the shell surface and thus cut through successive
709 shell layers. This situation is identical to that in *Mickwitzia* and *Setatella*. Horizontal, externally
710 open tubules that presumably housed marginal setae are sometimes found in *Mickwitzia* (Butler

et al., 2015) but in *Setatella*, only tubules situated on the pseudointerarea are open to the exterior. These tubules preserve longitudinal striations indicating that these perforations were also points of insertion for shell penetrating setae (Skovsted and Holmer, 2003; Skovsted et al., 2010). In *P. boreussinaensis*, the pseudointerareas of both valves exhibit similar externally open tubules inserted between and parallel to (or slightly oblique to) successive shell layers. Although no longitudinal striations were found in these tubules, the fact that previously formed shell laminae on the pseudointerarea sometimes exhibit cylindrical indentations in front of tubule openings (Figs. 10A$_6$ and 11B$_4$), strongly indicate that these tubules were originally occupied by stiff, needle-like objects extending from the shell. We interpret this as firm evidence for the presence of shell penetrating setae in *P. boreussinaensis.*

5. Biostratigraphic and palaeogeographic significance of early Cambrian brachiopods from North China

5.1 Biostratigraphic significance

Linguliform and some stem-group brachiopods (mickwitziids and eccentrothecimorph tommotiids) were important components of early Cambrian skeletal communities, and are common globally in fine siliciclastic and carbonate rocks from the early and middle Cambrian (Holmer et al., 1996; Holmer and Popov, 2000; Ushatinskaya and Holmer, 2001; Li and Holmer, 2004, Skovsted and Holmer, 2005; Ushatinskaya, 2008; Ushatinskaya and Korovnikov, 2014; Butler et al., 2015; Popov et al., 2015; Smith et al., 2015; 2016; Z.F. Zhang et al., 2015, 2016

732 and the references therein). However, the biostratigraphic significance of Cambrian
733 brachiopods is still not fully explored. Recently, Z.F. Zhang et al. (2016) gave a brief review of
734 the stratigraphic distribution of linguloids and acrotretoids across the known Cambrian
735 palaeocontinents, e.g. South China (Three Gorges area and eastern Yunnan Province), Australia,
736 Antarctica, Himalaya, Mongolia, Kazakhstan, Siberia and Laurentia (see reference listed in Z.F.
737 Zhang et al., 2016, p. 351) and pointed out that the first abundant occurrences of these
738 brachiopods constitute key evidence for an Cambrian Age 4 age while relatively little evidence
739 for diverse assemblages of these groups are available for older Cambrian strata Cambrian
740 Stages 2–3. The brachiopods from the lower Cambrian Xinji Formation in North China
741 comprise abundant linguloids (*Spinobolus* sp., *Eodicellomus* cf. *elkaniiformis*, *Eoobolus* sp. A,
742 *Eoobolus* sp. B) and one acrotretoid (*Eohadrotreta* cf. *zhenbaensis*). Previously, *Spinobolus* has
743 been restricted to the Shuijingtuo Formation (Stage 4) in Three Gorges area (Z.F. Zhang et al.,
744 2016), while *Eohadrotreta* has been reported from the Shuijingtuo Formation (Stage 4
745 according to Z.F. Zhang et al., 2016) in South China (Three Gorges area and Zhenba–Fangxian
746 region; Li and Holmer, 2004; Yang et al., 2015; Z.F. Zhang et al., 2016; Z.L. Zhang et al., 2016),
747 the Parahio Formation (Stage 4 to 5) in Himalaya (Popov et al., 2015) and the Mernmerna
748 Formation and Oraparinna Shale (uppermost Stage 3 to lowest Stage 4) in South Australia
749 (Betts et al., 2017; 2018). This provides strong indication that the brachiopod assemblage
750 described and illustrated herein may also belong to Stage 4. However, recent stratigraphic
751 studies of the early Cambrian in South Australia (Betts et al., 2016; 2017; 2018) indicate that
752 most of the main early Cambrian brachiopod groups, such as, the linguloids (e.g. *Eoobolus* sp.,

753 *Eodicellomus elkaniformiis* Holmer and Ushatinskaya, 2001 and *Kyrshabaktella davidii*
754 Holmer and Ushatinskaya, 2001), the botsfordiids (e.g. *Schizopholis yorkensis* (Holmer and
755 Ushatinskaya, 2001), *Curdus pararaensis* Holmer and Ushatinskaya, 2001 and *Minlatonia*
756 *tuckeri* Holmer and Ushatinskaya, 2001), the acrotretoids (*Vandalotreta djagoran* Kruse, 1990
757 and *Eohadrotreta*), the paterinides (*Askepasma toddense* Laurie, 1986) and the mickwitziids
758 (*Mickwitzia*, Skovsted et al., 2009) co-occurred in the *Dailyatia odyssei* zone (lower Stage 3 to
759 lower Stage 4). This indicates the brachiopods may already have been quite diverse and
760 abundant at some palaeocontinents in late Cambrian Stage 3 and should not be considered
761 restricted to Stage 4. This conforms with proposed stratigraphic correlation based on other small
762 shelly fossils and trilobites from North China (He et al., 1984; Li et al., 2014; Li et al., 2016;
763 Yun et al., 2016; Pan et al., 2017, 2018a, b and the references therein).
764
765 *5.2 Palaeogeographic significance*
766 The exact palaeogeographic position of the North China Platform in the Cambrian remains
767 controversial, depending on different methods of reconstruction. North China has been
768 variously placed as an independent continent close to the north of Australia according to
769 palaeobiogeographic comparisons (Brock et al., 2000; Golonka, 2011), located thousands of
770 kilometers to the east of Australia in the Palaeo-Pacific Ocean based on palaeomagnetic
771 interpretation (Li and Powell, 2001; Li et al., 2013), positioned far to the west of Gondwana
772 (Torsvik and Cocks 2013a, b, 2017) based on completely different interpretations of APWP data
773 for North China. However, McKenzie et al. (2011) instead suggested North China should be

774 part of the margin of Western Gondwana, bordering today's north-eastern India, based on
775 detrital zircon age distributions and Furongian polymerid trilobite biogeography while Han et
776 al. (2016) proposed that the North China craton collided with the northern Australian margin of
777 East Gondwana at ca. 500 Ma according to Zircon U-Pb and Hf isotopic data. More recently,
778 Pan et al. (2018a) argued that the strong similarity of the early Cambrian shelly fossil taxa
779 shared between North China and South Australia (most of the shelly fossil taxa have never been
780 found in India or other parts of Gondwana, see the references listed in Pan et al., 2018a). The
781 remarkable occurrence of endemic eccentrothecid tommotiid *Paterimitra pyramidalis* Laurie,
782 1986 in North China and Australia strongly suggests the southern margin of North China
783 Platform was closely juxtaposed to the north-eastern margin of Australian (East Gondwana)
784 during the early Cambrian.

785 As discussed above, the linguliform brachiopods had a wide geographic distribution during
786 the early and middle Cambrian. However, biogeographical analysis of early Cambrian
787 linguliform brachiopods have been significantly hampered by the low generic diversity of the
788 faunas and varying quality of taxonomic data (Popov et al., 2015). Recently, Popov et al. (2015)
789 tried to analyze the biogeographical affinity of Cambrian Stage 4 and 5 linguliform brachiopods.
790 The result for Stage 4 suggests that the main differences or links between the analyzed faunas
791 are defined by a few endemic or common taxa, respectively. In this analysis, South China and
792 South Kazakhstan are grouped as a separate cluster defined by the occurrence of *Lingulellotreta*
793 and *Palaeobolus* with low similarity to other faunas in Gondwana, Laurentia and Siberia. The
794 occurrence of *Schizopholis–Botsfordia* and *Eothele* define east Gondwana and Laurentian

795 faunas respectively and these are grouped together as a cluster separate from Siberia (Popov et
796 al., 2015). Actually, this result showed that biogeographical differentiation of the brachiopods
797 in Cambrian Stage 4 and 5 approximately follows the inferred relative position of the early
798 Palaeozoic continents during that time (Popov et al., 2015) which means that the
799 biogeographical relationships of the early Cambrian brachiopod fauna also shed lights on
800 palaeogeographic reconstructions. Due to lack of available early Cambrian brachiopod data at
801 the time, North China was not included in the analysis conducted by Popov et al. (2015).
802 Although, only seven genera, three species and four unidentified species of brachiopods from
803 the Shuiyu section are described here, they still provide a distinctive biogeographic signal.
804 *Eoobolus* is a brachiopod with worldwide distribution in Stage 4 and may have limited
805 biogeographical significance (Popov et al., 2015). However, the discovery of *Schizopholis*
806 *yorkensis* from North China may suggest North China also belong to the low latitude 'east'
807 Gondwana fauna (including South Australia, Antarctica and Himalaya) as argued by (Popov et
808 al., 2015). The co-occurrence of *Eohadrotreta* in South China, North China, Himalaya and
809 possibly South Australia provide additional evidence for this. The shared occurrence of
810 *Spinobolus* in North and South China suggests the faunal connections between these two areas,
811 although species determination of the specimens illustrated herein is still not definite.
812 Furthermore, the exclusive occurrence of *Askepasma toddense* and *Eodicellomus* cf.
813 *elkaniiformis* in North China and South Australia further strengthens the much closer
814 palaeobiogeographic connections between North China and South Australia. In general, the
815 early Cambrian brachiopod fauna from North China show a quite strong connection to east

Gondwana (South Australia, Himalaya, Antarctica and South China), with only one taxon, *Eoobolus*, with a wide distribution in the early Cambrian. The highest similarity is to brachiopod faunas of South Australia, which is consistent with the strong similarity among other shelly fossils in the associated assemblage (most of these taxa have never been found in Himalaya or South China) shared between these two regions (Pan et al., 2018a and the references therein). Thus, the palaeobiogeographic distribution of brachiopod fauna supports that the North China Platform was located close to current South Australia (East Gondwana) in the early Cambrian.

Acknowledgments

This work was supported by grants from the National Natural Science Foundation of China (41372021), the Chinese Academy of Sciences (XDB10010101, XDB18000000 and XDB18030304), the Ministry of Science and Technology of China (2013CB835000) and the Swedish Research Council (VR2016-04610). We thank Lanyun Miao and Changjun Sun (Nanjing) for their field guidance and assistance.

References

Balthasar, U., 2004. Shell structure, ontogeny and affinities of the Lower Cambrian bivalved problematic fossil *Mickwitzia muralensis* Walcott, 1913. Lethaia 37, 381–400.

Balthasar, U., Skovsted, C.B., Holmer, L.E., Brock, G.A., 2009. Homologous skeletal secretion in tommotiids and brachiopods. Geology 37, 1143–1146.

837 Bengtson, S., Morris, S.C., Cooper, B.J., Jell, P.A., Runnegar, B.N., 1990. Early Cambrian
838 fossils from South Australia. Memoirs of the Association of Australasia Palaeontologists 9,
839 1–364.
840 Betts, M.J., Paterson, J.R., Jago, J.B., Jacquet, S.M., Skovsted, C.B., Topper, T.P., Brock, G.A.,
841 2016. A new lower Cambrian shelly fossil biostratigraphy for South Australia. Gondwana
842 Research 36, 176–208.
843 Betts, M.J., Paterson, J.R., Jago, J.B., Jacquet, S.M., Skovsted, C.B., Topper, T.P., Brock, G.A.,
844 2017. Global correlation of the early Cambrian of South Australia: Shelly fauna of the
845 Dailyatia odyssei Zone. Gondwana Research 46, 240–279.
846 Betts, M.J., Paterson, J.R., Jacquet, S.M., Andrew, A.S., Hall, P.A., Jago, J.B., Jagodzinski, E.A.,
847 Preiss, W.V., Crowley, J.L., Brougham, T., Mathewson, C.P., García-Bellido, D.C., Topper, T.P.,
848 Skovsted, C.B., Brock, G.A. 2018. Early Cambrian chronostratigraphy and geochronology of
849 South Australia. Earth-Science Reviews 185, 498–543.
850 Brock, G.A., Cooper, B.J., 1993. Shelly fossils from the Early Cambrian (Toyonian) Wirrealpa,
851 Aroona Creek, and Ramsay limestones of South Australia. Journal of Paleontology, 758–
852 787.
853 Brock, G., Engelbretsen, M., Jago, J., Kruse, P., Laurie, J., Shergold, J., Shi, G., Sorauf, J., 2000.
854 Palaeobiogeographic affinities of Australian Cambrian faunas. Memoir of the Association
855 of Australasian Palaeontologists 23, 1–61.
856 Bureau of Geology and Mineral Resources of Shanxi Province, 1989. Regional Geology of
857 Shanxi Province. Beijing, Geological Publishing House, pp. 116–120 (in Chinese).

Butler, A.D., Streng, M., Holmer, L.E., Babcock, L.E., 2015. Exceptionally preserved *Mickwitzia* from the Indian Springs Lagerstätte (Cambrian Stage 3), Nevada. Journal of Paleontology 89, 933–955.

Chen, J.Y., Huang, D.Y., Chuang, S.H., 2007. Reinterpretation of the Lower Cambrian brachiopod *Heliomedusa orienta* Sun and Hou, 1987 as a discinid. Journal of Paleontology 81, 38–47.

Claybourn, T., 2017. Cambrian Series 2 (Stages 3–4) Small Shelly Fossils from East Antarctica. Licentiate thesis, Uppsala University, pp. 28 .

Dai, T., Zhang, X.L., 2012. Ontogeny of the trilobite Estaingia sinensis (Chang) from the lower Cambrian of South China. Bulletin of Geosciences 87, 151–158.

Devaere, L., Holmer, L., Clausen, S., Vachard, D., 2015. Oldest Mickwitziid Brachiopod from the Terreneuvian of Southern France. Acta Palaeontologica Polonica 60, 755–768.

Duméril, C., 1806. Zoologie analytique, ou Méthode naturelle de classification des animaux: rendue plus facile à l'aide de tableaux synoptiques. Allais (in French).

Fonin, V.D., Smirnova, T.N., 1967. New group of problematic Early Cambrian organisms and methods of preparing them. Paleontological Journal 2, 7–18.

Geyer, G., 1994. An enigmatic bilateral fossil from the Lower Cambrian of Morocco. Journal of Paleontology 68, 710–716.

Golonka, J., 2011. Phanerozoic palaeoenvironment and palaeolithofacies maps of the Arctic region. Geological Society, London, Memoirs 35, 79–129.

878 Gorjansky, V.J. 1969. Inarticulate brachiopods of the Cambrian and Ordovician of the northwest
879 Russian Platform. Ministerstvo Geologii RSFSR, Severo−Zapadnoe Territorialnoe
880 Geologičeskoe Upravlenie 6, 1–173 (in Russian).
881 Gorjansky, V.J., Popov, L.E., 1985. Morfologiya, systematicheskoye polozheniye i
882 proiskhozhdeniye bezzamkovykh breakhiopod s karbonatnoy rakovinoy.
883 Paleontologicheskiy Zhurnal 3, 3–14 (in Russian).
884 Gravestock, D.I., Alexander, E.M., Demidenko, Y.E., Esakova, N.B., Holmer, L.E., Jago, J.B.,
885 Lin, T.R., Melnikova, N., Parkhaev, P.Y., Rozanov, A.Y., Ushatinskaya, G.T., Zang, W.L.,
886 Zhegallo, E.A., Zhuravlev, A.Y., 2001. The Cambrian biostratigraphy of the Stansbury
887 Basin, South Australia. Transactions of the Palaeontological Institute of the Russian
888 Academy of Sciences 282, pp. 344.
889 Han, Y.G., Zhao, G.C., Cawood, P.A., Sun, M., Eizenhöfer, P.R., Hou, W.Z., Zhang, X.R., Liu,
890 Q., 2016. Tarim and North China cratons linked to northern Gondwana through switching
891 accretionary tectonics and collisional orogenesis. Geology 44, 95–98.
892 He, T.G., Pei, F., 1985. The discovery of bivalves from the lower Cambrian Xinji Formation in
893 Fangcheng county, Henan province. Journal of Chengdu College of Geology 1, 61–68 (in
894 Chinese, with English abstract).
895 He, T.G., Pei, F., Fu, G.H., 1984. Small shelly fossils from the lower Cambrian Xinji Formation
896 in Fangcheng County, Henan Province. Acta Palaeontologica Sinica 23, 350–357 (in
897 Chinese, with English abstract).

898 Holmer, L.E., Popov, L.E., 2000. Lingulata. In: Kaesler, R.L. (Ed.), Treatise on Invertebrate
899 Paleontology. The Geological Society of America and the University of Kansas, Boulder,
900 Colorado, and Lawrence, Kansas, pp. 30–146.
901 Holmer, L.E., Popov, L.E., 2007. Organophosphatic bivalved stem-group brachiopods. In:
902 Selden, P.A. (Ed.), Treatise on Invertebrate Paleontology, Part H, Brachiopoda, Revised,
903 Vol. 6. The Geological Society of America and the University of Kansas, Boulder, Colorado,
904 and Lawrence, Kansas, pp. 2580–2590.
905 Holmer, L.E., Popov, L.E., Wrona, R., 1996. Early Cambrian lingulate brachiopods from glacial
906 erratics of King George Island (South Shetland Islands), Antarctica. Palaeontologia
907 Polonica 55, 37–50.
908 Holmer, L.E., Popov, L.E., Streng, M., 2008a. Organophosphatic stem group brachiopods:
909 implications for the phylogeny of the subphylum Linguliformea. Fossils and Strata 54, 3–
910 11.
911 Holmer, L.E., Skovsted, C.B., Brock, G.A., Valentine, J.L., Paterson, J.R., 2008b. The Early
912 Cambrian tommotiid *Micrina*, a sessile bivalved stem group brachiopod. Biology Letters 4,
913 724–728.
914 Hsiang, L.W., 1963. Trilobita. In: Academy of Geological Sciences, Ministry of Geology (Ed.),
915 Fossil Atlas of Qinling Mountains. China Industry Press, Beijing, p. 27 (in Chinese).
916 Jago, J.B., Zang, W.L., Sun, X.W., Brock, G.A., Paterson, J.R., Skovsted, C.B., 2006. A review
917 of the Cambrian biostratigraphy of South Australia. Palaeoworld 15, 406–423.

King, W., 1846. Remarks on certain genera belonging to the class Paliobranchiata. Annals and Magazine of Natural History 18, 26–42.

Koneva, S.P., 1986. Some Middle and Late Cambrian inarticulate brachiopods in the Maly Karatau (southern Kazakhstan). Trudy Instituta Geologii i Geofiziki, Akademiya Nauk SSSP, Sibirskoye Otdelenye 669, 201–209.

Kouchinsky, A.V., Bengtson, S., 2017. X-ray tomographic microscopy tightens affinity of the early Cambrian *Oymurania* to the brachiopod stem group. Palaeontologia Polonica 62, 39–43.

Kouchinsky, A.V., Holmer, L.E., Steiner, M., Ushatinskaya, G.T., 2015. The new stem-group brachiopod *Oymurania* from the lower Cambrian of Siberia. Acta Palaeontologica Polonica 60, 963–980.

Kruse, P.D., 1990. Cambrian palaeontology of the Daly Basin. Darwin, Government Printer of the Northern Territory, pp. 1–58.

Kuhn, O., 1949. Lehrbuch der Paläozoologie. Schweizerbart, Stuttgart, pp.1–326 (in Russian).

Landing, E., Geyer, G., Bartowski, K.E., 2002. Latest Early Cambrian small shelly fossils, trilobites, and Hatch Hill dysaerobic interval on the Québec continental slope. Journal of Paleontology 76, 287–305.

Laurie, J.R., 1986. Phosphatic fauna of the Early Cambrian Todd River Dolomite, Amadeus Basin, Central Australia. Alcheringa 10, 431–454.

937 Lee, S., 1978. Trilobite, In: Southwest Institute of Geological Sciences, ed., Palaeontological
938 Atlas of Southwest China, Sichuan Volume, Part 1, from Sinian to Devonian. Beijing,
939 Geological Publishing House, 180 (in Chinese).
940 Li, G.X., Holmer, L.E., 2004. Early Cambrian lingulate brachiopods from the Shaanxi Province,
941 China. GFF 126, 193–211.
942 Li, G.X., Zhang, Z.F., Hua, H., Yang, H.N., 2014. Occurrence of the enigmatic bivalved fossil
943 Apistoconcha in the lower Cambrian of southeast Shaanxi, North China Platform. Journal
944 of Paleontology 88, 359–366.
945 Li, L.Y., Zhang, X.L., Yun, H., Li, G.X., 2016. New occurrence of Cambroclavus absonus from
946 the lowermost Cambrian of North China and its stratigraphical importance. Alcheringa: An
947 Australasian Journal of Palaeontology 40, 45–52.
948 Li, L.Y., Zhang, X.L., Yun, H., Li, G.X., 2017. Complex hierarchical microstructures of
949 Cambrian mollusk Pelagiella: insight into early biomineralization and evolution. Scientific
950 reports 7, 1935.
951 Li, Z.X., Powell, C.McA., 2001. An outline of the palaeogeographic evolution of the
952 Australasian region since the beginning of the Neoproterozoic. Earth-Science Reviews 53,
953 237–277.
954 Li, Z.X., Evans, D.A., Halverson, G.P., 2013. Neoproterozoic glaciations in a revised global
955 palaeogeography from the breakup of Rodinia to the assembly of Gondwanaland.
956 Sedimentary Geology 294, 219–232.

957 Liu, Q., Ma, L.F., Zhu, Y.H., Jin, R.G., Dai, W.S., Chen, Y.H., Fan, X.H., Zhang, T.G., Zhang,
958 Z.J., 1994. Lithofacies palaeogeography and gypsum deposits of the lower Cambrian of
959 North China platform. Geologic Publishing House, Beijing, pp. 1–144 (in Chinese)
960 Liu, Y.H., 1986. The lower Cambrian Xinji Formation in Hennan Province. Henan Geology 4,
961 28–35 (in Chinese).
962 Liu, Y.H., P., W.J., Zhang, H.Q., Du, F.J., 1991. The Cambrian and Ordovician Systems of
963 Henan Province. Geological Publishing House, Beijing. pp. 1–225 (in Chinese).
964 Lu, Y.H., Zhang, W.T., Zhu, Z.L., Qian, Y., Xiang, L.W., 1965. The Trilobites of China. Science
965 Press, Beijing, p. 85 (in Chinese).
966 Matthew, G.F., 1902. Notes on Cambrian faunas. Royal Society of Canada Transactions (Ser. 2,
967 Sect. 4) 8, 93–112
968 McKenzie, N.R., Hughes, N.C., Myrow, P.M., Choi, D.K., Park, T.Y., 2011. Trilobites and
969 zircons link North China with the eastern Himalaya during the Cambrian. Geology 39, 591–
970 594.
971 Miao, L.Y., 2014. Biostratigraphy of the Basal Cambrian Xinji Formation and the Houjiashan
972 Formation From the Southern North China Platform. Master thesis, University of Chinese
973 Academy of Sciences (in Chinese, with English summary).
974 Miao, L.Y., Zhu, M.Y., 2014. Trace fossils from the basal Cambrian Xinji Formation in
975 Southern North China Platform and its chronological significance. Acta Palaeontologica
976 Sinica 53, 274–289 (in Chinese, with English abstract).

977 Pan, B., Miao, L., Yang, H., Li, G., 2015. Enigmatic tubular fossil Cupitheca from the lower
978 Cambrian Xinji Formation of Luonan, Shaanxi Province. Acta Micropalaeontologica Sinica
979 32, 384–395 (in Chinese, with English abstract).
980 Pan, B., Skovsted, C.B., Sun, H.J., Li, G.X., 2017. Hyoliths from the lower Cambrian along the
981 southern margin of the North China Platform and their biostratigraphic and
982 palaeogeographic significances. In: Yang, Q., Reitner, J., Wang, Y.D., Reich, M. (Eds.),
983 Critical Intervals in Earth History: Palaeobiological Innovations, Abstract Volume of the
984 2nd Joint Conference Palaeontological Society of China and the Paläontologische
985 Gesellschaft, pp. 249–250.
986 Pan, B., Brock, G.A., Skovsted, C.B., Betts, M.J., Topper, T.P., Li, G., 2018a. *Paterimitra*
987 *pyramidalis* Laurie, 1986, the first tommotiid discovered from the early Cambrian of North
988 China. Gondwana Research 63, 179–185.
989 Pan, B., Topper, T.P., Skovsted, C.B., Miao, L., Li, G., 2018b. Occurrence of *Microdictyon* from
990 the lower Cambrian Xinji Formation along the southern margin of the North China Platform.
991 Journal of Paleontology 92, 59–70.
992 Paterson, J.R., Brock, G.A., 2007. Early Cambrian trilobites from Angorichina, Flinders Ranges,
993 South Australia, with a new assemblage from the Pararaia bunyerooensis Zone. Journal of
994 Paleontology 81, 116–142.
995 Paterson, J.R., Jago, J.B., Gehling, J.G., García-Bellido, D.C., Edgecombe, G.D., Lee, M.S.,
996 Rábano, I., Gozalo, R., García-Bellido, D., 2008. Early Cambrian arthropods from the Emu

997 Bay Shale Lagerstätte, South Australia. Advances in trilobite research. Cuadernos del
998 Museo Geominero 9, 319–325.
999 Peng, J., Zhao, Y.L., Qin, Q., Yan, X., Ma, H.T., 2010. New material of brachiopods from the
1000 Qiandongian (Lower Cambrian) Balang Formation, eastern Guizhou, South China. Acta
1001 Palaeontologica Sinica 49, 372–379 (in Chinese, with English abstract).
1002 Percival, I.G., Kruse, P.D., 2014. Middle Cambrian brachiopods from the southern Georgina
1003 Basin of central Australia. Memoirs of the Association of Australasian Palaeontologists,
1004 349–402.
1005 Popov, L.E., Holmer, L.E., Hughes, N.C., Ghobadi Pour, M., Myrow, P.M., 2015. Himalayan
1006 Cambrian brachiopods. Papers in Palaeontology 1, 345–399.
1007 Rowell, A.J., 1965. Inarticulata. In: Moore, R.C. (Ed.), Treatise on Invertebrate Paleontology,
1008 Part H, Brachiopoda, H260–H296. Geological Society of America and University of Kansas
1009 Press, Boulder.
1010 Rowell, A.J., 1977. Early Cambrian brachiopods from the southwestern Great Basin of
1011 California and Nevada. Journal of Paleontology 51, 68–85.
1012 Schindewolf, O.H., 1955. Über einige kambrische Gattungen inartikulater Brachiopoden.
1013 Neues Jahrbuch für Mineralogie, Geologie und Paläontologie 12, 538–557.Schuchert, C.,
1014 1893. A classification of the Brachiopoda. American Geologist 11, 141–167 (in German).
1015 Schmidt, F. 1888. Über eine neuentdeckte untercambrische Fauna in Estland. Académie
1016 Impériale des Sciences, St Petersbourg, Mémoires (series 7) 36, 1–27.
1017 Schuchert, C. 1893. A classification of the Brachiopoda. American Geologist 11, 141–167.

1018 Skovsted, C.B., Holmer, L.E., 2003. The Early Cambrian (Botomian) stem group brachiopod
1019 Mickwitzia from North-east Greenland. Acta Palaeontologica Polonica 48, 1–20.
1020 Skovsted, C.B., Holmer, L.E., 2005. Early Cambrian brachiopods from North-East Greenland.
1021 Palaeontology 48, 325–345.
1022 Skovsted, C.B., 2006a. Small Shelly fauna from the upper Lower Cambrian Bastion and Ella
1023 Island formations, North-East Greenland. Journal of Paleontology 80, 1087–1112.
1024 Skovsted, C.B., 2006b. Small shelly fossils from the basal Emigrant Formation (Cambrian,
1025 uppermost Dyeran Stage) of Split Mountain, Nevada. Canadian Journal of Earth Sciences
1026 43, 487–496.
1027 Skovsted, C.B., Holmer, L.E., 2006. The Lower Cambrian brachiopod Kyrshabaktella and
1028 associated shelly fossils from the Harkless Formation, southern Nevada. GFF 128, 327–337.
1029 Skovsted, C.B., Peel, J.S., 2010. Early Cambrian brachiopods and other shelly fossils from the
1030 basal Kinzers Formation of Pennsylvania. Journal of Paleontology 84, 754–762.
1031 Skovsted, C.B., Brock, G., Holmer, L., Paterson, J., 2009. First report of the early Cambrian
1032 stem group brachiopod *Mickwitzia* from East Gondwana. Gondwana Research 16, 145–150.
1033 Skovsted, C.B., Streng, M., Knight, I., Holmer, L., 2010. Setatella significans, a new name for
1034 mickwitziid stem group brachiopods from the lower Cambrian of Greenland and Labrador.
1035 GFF 132, 117–122.
1036 Skovsted, C.B., Clausen, S., Alvaro, J.J., Ponleve, D., 2014. Tommotiids from the early C
1037 ambrian (S eries 2, S tage 3) of M orocco and the evolution of the tannuolinid scleritome
1038 and setigerous shell structures in stem group brachiopods. Palaeontology 57, 171–192.

1039 Skovsted, C.B., Ushatinskaya, G., Holmer, L.E., Popov, L.E., Kouchinsky, A., 2015. Taxonomy,
1040 morphology, shell structure and early ontogeny of *Pelmanotreta* nom. nov. from the lower
1041 Cambrian of Siberia. GFF 137, 1–8.
1042 Skovsted, C.B., Pan, B., Topper, T.P., Betts, M.J., Li, G.X., Brock, G.A., 2016. The operculum
1043 and mode of life of the lower Cambrian hyolith Cupitheca from South Australia and North
1044 China. Palaeogeography, Palaeoclimatology, Palaeoecology 443, 123–130.
1045 Skovsted, C.B., Knight, I., Balthasar, U., Boyce, W.D., 2017. Depth related brachiopod faunas
1046 from the lower Cambrian Forteau Formation of southern Labrador and western
1047 Newfoundland, Canada. Palaeontologia Electronica 20, 1–52.
1048 Smith, P.M., Brock, G.A., Paterson, J.R., 2015. Fauna and biostratigraphy of the Cambrian
1049 (Series 2, Stage 4; Ordian) Tempe Formation (Pertaoorrta Group), Amadeus Basin,
1050 Northern Territory. Alcheringa 39, 40–70.
1051 Smith, P.M., Brock, G.A., Paterson, J.R., 2016. Linguliformean brachiopods from the early
1052 Templetonian (Cambrian series 3, stage 5) Giles Creek Dolostone, Amadeus Basin,
1053 Northern territory. Australasian Palaeontological Memoirs, 125–143.
1054 Sun, W.G., Hou, X.G., 1987. Early Cambrian medusae from Chengjiang, Yunnan, China. Acta
1055 Palaeontologica Sinica 26, 299–305 (in Chinese, with English Abstract).
1056 Topper, T.P., Brock, G.A., Skovsted, C.B., Paterson, J.R., 2009. Shelly fossils from the lower
1057 Cambrian Pararaia bunyerooensis Zone, Flinders Ranges, South Australia. Memoirs of the
1058 Association of Australasian Palaeontologists 37, 199–246.

1059 Topper, T.P., Holmer, L.E., Skovsted, C.B., Brock, G.A., Balthasar, U., Larsson, C.M., Stolk,
1060 S.P., Harper, D.A., 2013. The oldest brachiopods from the lower Cambrian of South
1061 Australia. Acta Palaeontologica Polonica 58, 93–109.
1062 Torsvik, T.H., Cocks, L.R.M., 2013a. Gondwana from top to base in space and time. Gondwana
1063 Research 24, 999–1030.
1064 Torsvik, T.H., Cocks, L.R.M., 2013b. New global palaeogeographical reconstructions for the
1065 Early Palaeozoic and their generation. Geological Society, London, Memoirs 38, 5–24.
1066 Torsvik, T.H., Cocks, L.R.M., 2017. Earth history and palaeogeography. Cambridge University
1067 Press, UK, pp. 85–100.
1068 Ushatinskaya, G.T., 2008. Origin and dispersal of the earliest brachiopods. Paleontological
1069 Journal 42, 776–791.
1070 Ushatinskaya, G. T., Holmer, L. E. 2001. Brachiopods. 120–132. In Gravestock, D.I., Alexander,
1071 E.M., Demidenko, Y.E., Esakova, N.B., Holmer, L.E., Jago, J.B., Lin, T.R., Melnikova, N.,
1072 Parkhaev, P.Y., Rozanov, A.Y., Ushatinskaya, G.T., Zang, W.L., Zhegallo, E.A., Zhuravlev,
1073 A.Y., 2001. The Cambrian biostratigraphy of the Stansbury Basin, South Australia.
1074 Transactions of the Palaeontological Institute of the Russian Academy of Sciences 282, pp.
1075 344.
1076 Ushatinskaya, G.T., Korovnikov, I.V., 2014. Revision of the Early-Middle Cambrian Lingulida
1077 (Brachiopoda) from the Siberian Platform. Paleontological Journal 48, 26–40.

Ushatinskaya, G.T., Korovnikov, I.V., 2016. Revision of the superfamily Acrotheloidea (Brachiopoda, class Linguliformea, order Lingulida) from the Lower and Middle Cambrian of the Siberian Platform. Paleontological Journal 50, 450–462.

Waagen, W., 1885. Salt Range fossils, vol. 1, part 4. Productus Limestone fossils, Brachiopoda. Palaeontologia Indica, Ser. 13, 4, 611–728.

Walcott, C.D., 1908. Cambrian Brachiopoda and Paleontology, pt. 3 – Cambrian Brachiopoda, descriptions of new genera and species. Smithsonian Miscellaneous Collections 53, 53–137

Williams, A., Carlson, S.J., Brunton, C.H.C., Holmer, L.E., Popov, L., 1996. A supra-ordinal classification of the Brachiopoda. Phil. Trans. R. Soc. Lond. B 351, 1171–1193.

Williams, A., Popov, L.E., Holmer, L.E., Cusack, M., 1998. The diversity and phylogeny of the paterinate brachiopods. Palaeontology 41, 221–262.

Xiao, L.G., Zhou, B.H., 1984. Early Cambrian hyolitha from Huainan and Huoqiu county in Anhui province. Professional Papers of Stratigraphy and Palaeontology, Chinese Academy of Geological Sciences 13, 141–151 (in Chinese, with English abstract).

Yang, B., Steiner, M., Keupp, H., 2015. Early Cambrian palaeobiogeography of the Zhenba–Fangxian Block (South China): independent terrane or part of the Yangtze Platform? Gondwana Research 28, 1543–1565.

Yu, W., Xu, J., Yi, K., 1984. Discovery of molluscan fauna from lower Cambrian Xinji Formation of Luonan, Shannxi. Journal of Stratigraphy 8, 234 (in Chinese, with English abstract).

1098 Yuan, J.L., Zhu, X.J., Lin, J.P., Zhu, M.Y., 2011. Tentative correlation of Cambrian Series 2
1099 between South China and other continents. Bulletin of Geosciences 86, 397–404.
1100 Yun, H., Zhang, X., Li, L., Zhang, M., Liu, W., 2016. Skeletal fossils and microfacies analysis
1101 of the lowermost Cambrian in the southwestern margin of the North China Platform. Journal
1102 of Asian Earth Sciences 129, 54–66.
1103 Zhang, W.T., Zhu, Z.L., 1979. Notes on some trilobites from lower Cambrian Houjiashan
1104 Formation in southern and southwestern parts of North China. Acta Palaeontologica Sinica
1105 18, 513–529 (in Chinese).
1106 Zhang, W.T., Li, J.J., Qian, Y.Y., Zhu, Z.L., Chen, C.Z., Zhang, S.X., 1957. Cambrian and
1107 Ordovician strata of East Gorges, Hubei. Bulletin of Sciences 5, 145–146 (in Chinese).
1108 Zhang, W.T., Zhu, Z.L., Yuan, K.X., Lin, H.L., Qian, Y., H.J., W., Yuan, J.L., 1979. The
1109 boundary of the Cambrian-upper Precambrian in the southern and southwestern parts of
1110 North China. Acta Stratigraphica Sinica 3, 51–56 (in Chinese).
1111 Zhang, W.T., Lu, Y.H., Zhu, Z.L., Qian, Y.Y., Lin, H.L., Zhou, Z.Y., Zhang, S.G., Yuan, J.L.
1112 1980. Cambrian trilobite faunas of southwestern China. Palaeontologia Sinica 159, New
1113 Series 16, 1–497 (in Chinese, with English summary).
1114 Zhang, Z.F., Li, G.X., Emig, C.C., Han, J., Holmer, L.E., Shu, D.G., 2009. Architecture and
1115 function of the lophophore in the problematic brachiopod *Heliomedusa orienta* (Early
1116 Cambrian, South China). Geobios 42, 649–661.

Zhang, Z.F., Zhang, Z.L., Li, G.X., Holmer, L.E., 2015. First report of linguloid brachiopods with soft parts from the lower Cambrian (Series 2, Stage 4) of the Three Gorges area, South China, Annales de Paléontologie. Elsevier, pp. 167–177.

Zhang, Z.F., Zhang, Z.L., Li, G.X., Holmer, L.E., 2016. The Cambrian brachiopod fauna from the first-trilobite age Shuijingtuo Formation in the Three Gorges area of China. Palaeoworld 25, 333–355.

Zhang Z.L., 2018. Early Cambrian Phosphatic-shelled brachiopods from South China. Northwest University (PhD thesis).

Zhang, Z.L., Zhang, Z.F., Wang, H.Z., 2016. Epithelial cell moulds preserved in the earliest acrotretid brachiopods from the Cambrian (Series 2) of the Three Gorges area, China. GFF 138, 455–466.

Zhang, Z.L., Popov, L.E., Holmer, L.E., Zhang, Z.F., 2018a. Earliest ontogeny of early Cambrian acrotretoid brachiopods—first evidence for metamorphosis and its implications. BMC evolutionary biology 18, 1–15.

Zhang, Z.L., Zhang, Z.F., Holmer, L.E., Chen, F.Y., 2018b. Post-metamorphic allometry in the earliest acrotretoid brachiopods from the lower Cambrian (Series 2) of South China, and its implications. Palaeontology 61, 183–207.

Zhou, B.H., Xiao, L.G., 1984. Early Cambrian monoplacophorans and gastropods from Huainan and Huoqiu Counties (Anhui Provence). Professional Papers of Stratigraphy and Palaeontology 13, 125–140 (in Chinese, with English abstract).

1138 Figure captions

1139

1140 Fig. 1. Locality map and lithostratigraphic column for the Shuiyu section. Abbreviations: LQ
1141 F., Luoquan Formation; LJY F., Longjiayuan Formation.

1142

1143 Fig. 2. *Askepasma toddense Laurie*, 1986 from the early Cambrian Xinji Formation, Shuiyu
1144 section, Ruicheng County, Shanxi Province. (A–E) dorsal valves; (A) NIGPAS168715, dorsal
1145 view; (A_1) posterolateral view of dorsal exterior; (B and B_1) NIGPAS168716; (B) dorsal view;
1146 (B_1) dorsal metamorphic shell; (C) NIGPAS168717, posterior view; (D and D_1)
1147 NIGPAS168718; (D) interior view; (D_1) magnification of inner surface to show tiny spherical
1148 grains; (E and E_1) NIGPAS168719; (E) posterior view; (E_1) posterodorsal view to show
1149 homeochilidium and metamorphic shell; (F–H) ventral valves; (F) NIGPAS168720, ventral
1150 view; (F_1) posterodorsal view; (F_2) magnification of (F_1) to show pedicle callist and
1151 metamorphic shell; (G) NIGPAS168721, posterodorsal view; (G_1) dorsal view; (H–H_3)
1152 NIGPAS168722; (H) posterolateral view of dorsal exterior; (H_1) magnification of square in (H_2)
1153 to show the microscopic polygonal pits; (H_3) magnification of square in (H_2) to show the
1154 concentric growth ribs cut by short groove.

1155

1156 Fig. 3. *Eohadrotreta* cf. *zhenbaensis* Li and Holmer, 2004 from the early Cambrian Xinji
1157 Formation, Shuiyu section, Ruicheng County, Shanxi Province. (A–D) ventral valves; (A–A_3)
1158 NIGPAS168723; (A) ventral view; (A_1) lateral view of dorsal exterior; (A_2) posterior view; (A_3)

magnification of furrow bisecting the intertrough; (B–B_2) NIGPAS168724; (B) interior view; (B_1) lateral view of inner side; (B_2) weakly preserved apical process and epithelial cell moulds; (C–C_2) NIGPAS168725; (C) posterodorsal view; (C_1) magnification of pedicle foramen; (C_2) microscopic pitted ornament of ventral metamorphic shell; (D–D_1) NIGPAS168726; (D) dorsal view; (D_1) magnification of concentric fila interrupted by fold or drape-like nick points; (E–H) dorsal valves; (E–E_2) NIGPAS168727; (E) inner view; (E_1) lateral view of inner surface; (E_2) magnification of square in (E_1) to show the weak submedian ridges; (F–F_1) NIGPAS168728; (F) dorsal view; (F_1) microscopic pitted ornament of dorsal metamorphic shell; (G–G_1) NIGPAS168729; (G) anterior view of inner side; (G_1) magnification of dorsal pseudointerarea and median buttress; (H–H_1) NIGPAS168730; (H) anterolateral view of inner surface; (H_1) magnification of epithelial cell moulds.

Fig. 4. *Spinobolus* sp. from the early Cambrian Xinji Formation, Shuiyu section, Ruicheng County, Shanxi Province. (A–A_4) NIGPAS168731, dorsal valve; (A) dorsal view; (A_1) magnification of concentric ornament; (A_2) magnification of rounded pustules; (A_3) internal view; (A_4) posterolateral internal view.

Fig. 5. Ventral valves of *Eodicellomus* cf. *elkaniiformis* Holmer and Ushatinskaya, 2001 from the early Cambrian Xinji Formation, Shuiyu section, Ruicheng County, Shanxi Province. (A–A_2) NIGPAS168741; (A) posterolateral view; (A_1) posterior view; (A_2) anterolateral view of interior; (B–B_2) NIGPAS168742; (B) lateral view; (B_1) ventral view; (B_2) internal view; (C–C_2)

NIGPAS168743; (C) posterolateral view; (C_1) microscopic pits of metamorphic shell ornament; (C_2) ventral view; (D) NIGPAS168744, dorsolateral view of metamorphic shell; (E–E_1) NIGPAS168745; (E) posterolateral view of the interior; (E_1) internal view; (F) NIGPAS168746, ventral view; (G) NIGPAS168747, ventral view; (H–H_1) NIGPAS16878; (H) internal view; (H_1) anterior view of interior; (I–I_1) NIGPAS168749; (I) anterolateral view of interior; (I_1) magnification of the broken shell; (J) NIGPAS168750, anterior view of pseudointerarea.

Fig.6. Dorsal valves of *Eodicellomus* cf. *elkaniiformis* Holmer and Ushatinskaya, 2001 from the early Cambrian Xinji Formation, Shuiyu section, Ruicheng County, Shanxi Province. (A–A_1) NIGPAS168751; (A) internal view of the posterior part of adult dorsal shell; (A_1) dorsal view; (B–B_3) NIGPAS168752; (B) posterior view; (B_1) posterodorsal view; (B_2) internal view; (B_3) lateral view of the interior; (C–C_3) NIGPAS168753; (C) internal view; (C_1) dorsal view; (C_2) anterolateral view; (D) NIGPAS168754, microscopic pits of dorsal metamorphic shell ornament; (E–E_2) NIGPAS168755; (E) anterolateral view of the interior; (E_1) dorsal view; (E_2) enlargement of metamorphic shell ornament to show the lobes (the black circle); (F) NIGPAS168756, dorsal view.

Fig. 7. *Eoobolus* sp. A from the early Cambrian Xinji Formation, Shuiyu section, Ruicheng County, Shanxi Province. (A and D) ventral valves; (A–A_2) NIGPAS168732; (A) lateral view of internal surface; (A_1) inner view, wide arrows indicating pedicle nerves, narrow arrows indicating divergent *vascula lateralia*; (A_2) magnification of pedicle groove; (D–D_2)

NIGPAS168735; (D) ventral view; (D_1) magnification of the posterior ventral valve; (D_2) magnification of smooth concentric growth lines; (B and C) articulated valves; (B–B_1) NIGPAS168733; (B) dorsolateral view; (B_1) posterodorsal view; (C–C_2) NIGPAS168734; (C) ventral view; (C_1) microscopic pitted ornament of ventral metamorphic shell; (C_2) magnification of post-metamorphic shell ornament of juvenile ventral valve to show the concentric growth lines dashed by radial narrow lines; (E–G) dorsal valves; (E–E_3) NIGPAS168736; (E) dorsal view; (E_1) magnification of pustules; (E_2) magnification of smooth concentric growth lines; (E_3) internal view; (F–F_1) NIGPAS168737; (F) internal view, arrows indicating *vascula lateralia*; (F_1) posterolateral view; (G–G_1) NIGPAS168738; (G) posterolateral view; (G_1) dorsal view; (H) NIGPAS168739, anterolateral internal view.

Fig. 8. *Eoobolus* sp. B from the early Cambrian Xinji Formation, Shuiyu section, Ruicheng County, Shanxi Province. (A–A_3) ventral valve, NIGPAS168740; (A) internal view; (A_1) ventral view; (A_2) magnification of pustules; (A_3) anterolateral view.

Fig.9. *Schizopholis yorkensis* (Holmer and Ushatinskaya, 2001) from the early Cambrian Xinji Formation, Shuiyu section, Ruicheng County, Shanxi Province. (A–C) ventral valves. (A–A_3) NIGPAS168757; (A) posterior view; (A_1) posterior view of metamorphic shell and pseudointerarea; (A_2) ventral view of metamorphic shell; (A_3) internal view of pseudointerarea. (B–B_2) NIGPAS168758; (B) ventral view; (B_1) microscopic pits of metamorphic shell

1222 ornament; (B_2) pustules and concentric growth lines. (C) NIGPAS168759, internal view. (D and
1223 D_1) dorsal valve, NIGPAS168760; (D) internal view; (D_1) laterodorsal view. (E) articulated
1224 valve, NIGPAS168761, posterodorsal view.
1225
1226 Fig.10. Ventral valves of *Paramickwitzia boreussinaensis* n. gen. n. sp. Pan and Skovsted from
1227 the early Cambrian Xinji Formation, Shuiyu section, Ruicheng County, Shanxi Province. (A–
1228 A_{10}), NIGPAS168762; (A) posterior view; (A_1) anteroventral view; (A_2) ventral view; (A_3)
1229 dorsal view of pseudointerarea; (A_4) lateroventral view; (A_5) magnification of larger white
1230 rectangle in (A_4); (A_6) magnification of smaller black rectangle in (A_4); (A_7) magnification of
1231 larger white rectangle in (A_1); (A_8) magnification of smaller black rectangle in (A_1); (A_9 and
1232 A_{10}) metamorphic shell. (B–B_4), NIGPAS168763; (B) lateroventral view; (B_1) anterior view to
1233 show interior of pseudointerarea; (B_2) ventral view; (B_3) ventral view of metamorphic shell;
1234 (B_4) magnification of rectangle in (B_1).
1235
1236 Fig.11. Dorsal valves and fragmental shells of *Paramickwitzia boreussinaensis* n. gen. n. sp.
1237 Pan and Skovsted from the early Cambrian Xinji Formation, Shuiyu section, Ruicheng County,
1238 Shanxi Province. (A and B) dorsal valve. (A–A_2) NIGPAS168764; (A) posterodorsal view; (A_1)
1239 dorsal view; (A_2) metamorphic shell, arrows to show the lobes, circle to show the possible
1240 protegulum. (B–B_5) Holotype, NIGPAS168765; (B) dorsolateral view; (B_1) ventral view of
1241 pseudointerarea; (B_2) lateroposterior view of pseudointerarea; (B_3) anterior view to show
1242 interior of pseudointerarea; (B_4) posteroventral view of pseudointerarea; (B_5) dorsal view. (C

and D) shell fragments. (C and C_1) NIGPAS168766; (C) internal surface with numerous cones; (C_1) magnification of cones. (D and D_1) NIGPAS168767; (D) exterior surface with radial and concentric ornaments; (D_1) magnification of pustules.

A

N

Beijing

Shanxi
Province

600Km

South
China
Sea

500Km

110° 37′

Yuncheng
City

Yongji
County

Shuiyu
section

34° 46′

Ruicheng
County

Huang
River

B

(m)

(Unexposed)

Cambrian

Xinji Formation

Precambrian

LQ F.

LJY F.

10.7

7.7

6.9

4. 2

1.2

0

-6

-8.5

fossil horizon

feldspar-quartz sandstone

sandy limestone

conglomerates

phosphorous quartz siltstone

sandy dolostone

phosphrous pebbly siltstone

dolostone

anagenites

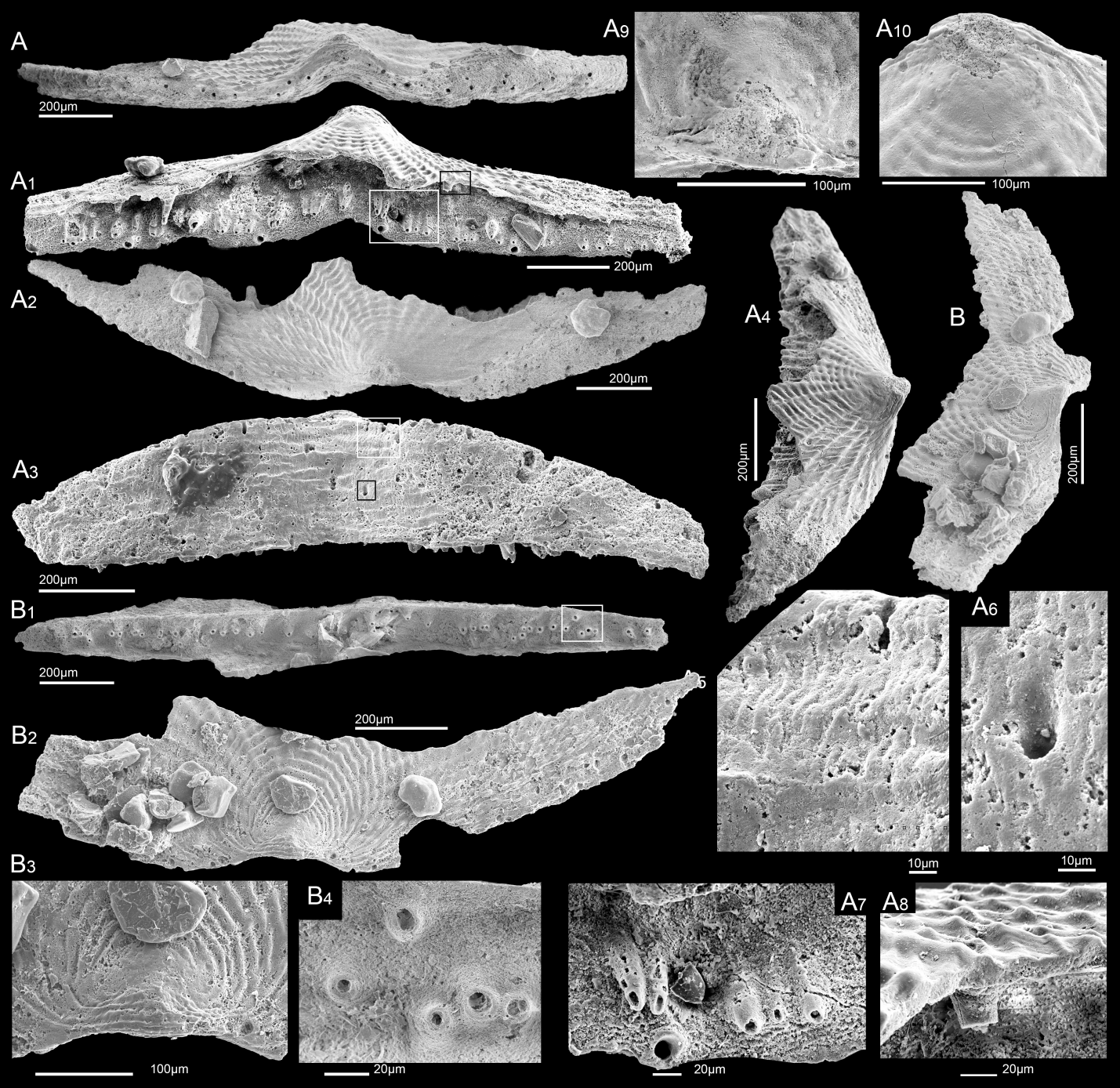
A
200μm
A9
100μm
A10
100μm
A1
200μm
A2
200μm
A4
200μm
B
200μm
A3
200μm
B1
200μm
B2
200μm
A6
10μm
10μm
B3
100μm
B4
20μm
A7
20μm
A8
20μm

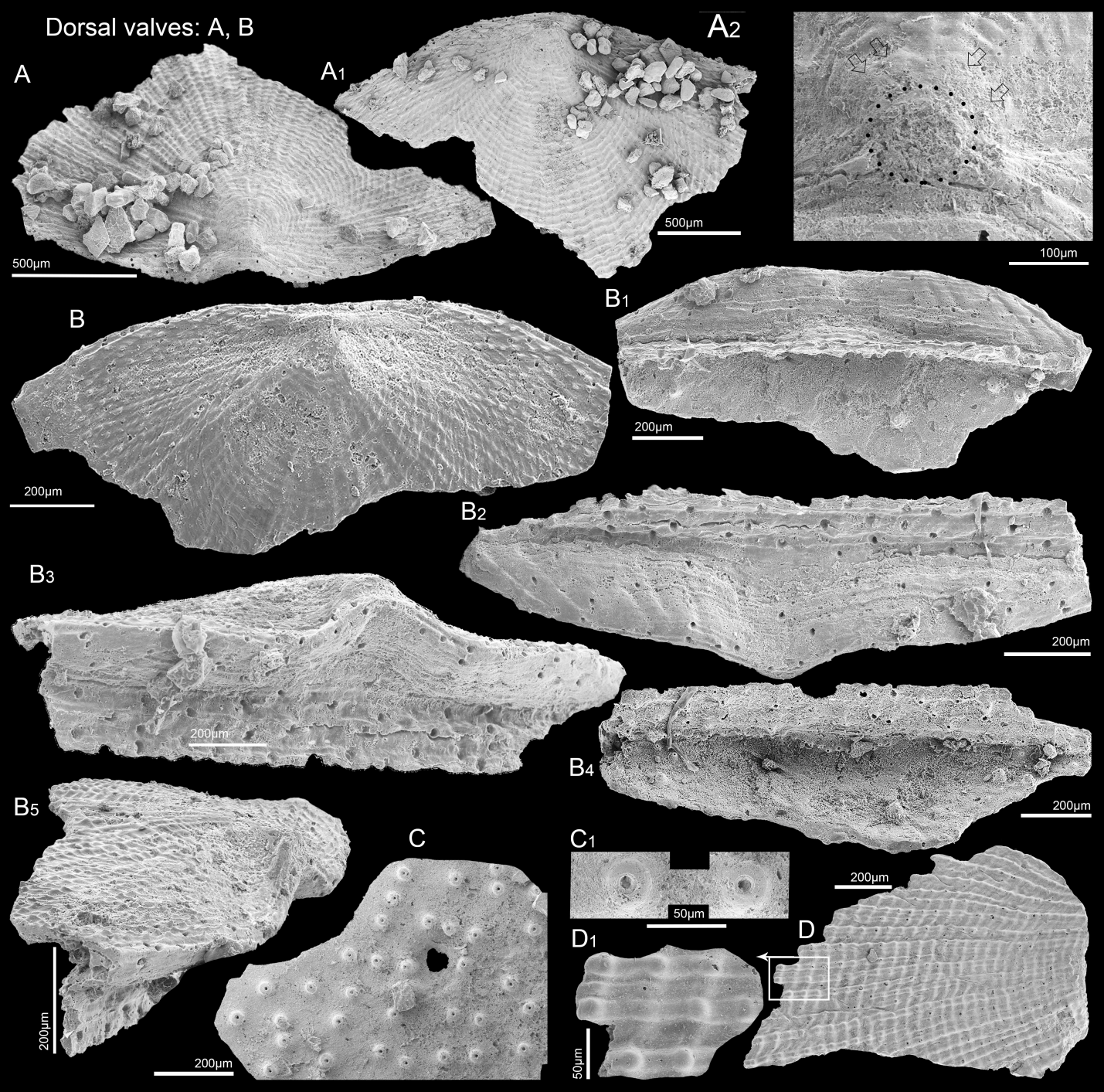
Dorsal valves: A, B
A
A1
A2
500µm
500µm
100µm
B
B1
200µm
200µm
B2
200µm
B3
200µm
B4
200µm
B5
C
C1
50µm
200µm
D
D1
200µm
200µm
50µm

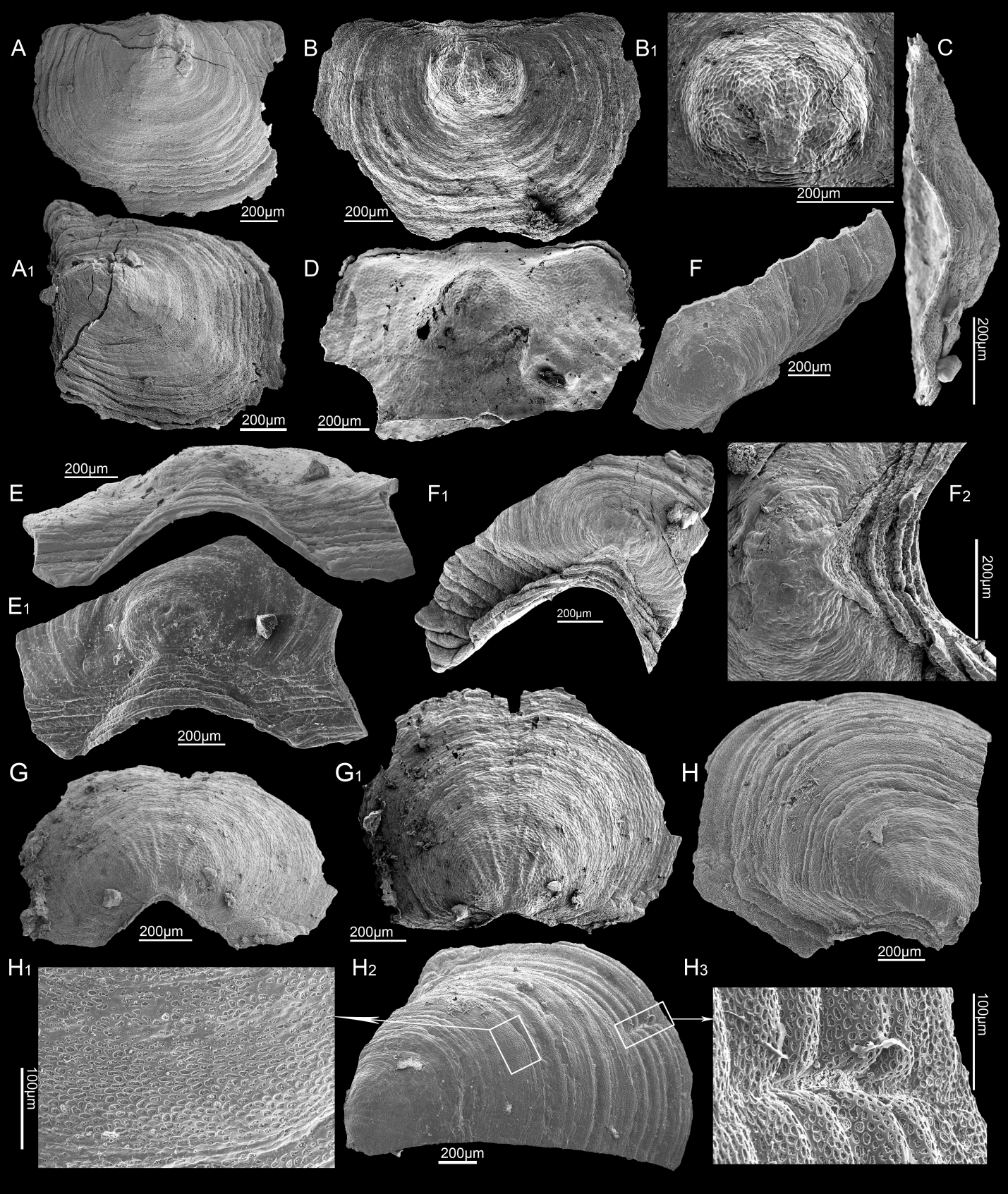
A
200μm
B
200μm
B1
200μm
C
200μm
A1
200μm
D
200μm
F
200μm
200μm
E
E1
200μm
F1
200μm
F2
200μm
G
200μm
G1
200μm
H
200μm
H1
100μm
H2
200μm
H3
100μm

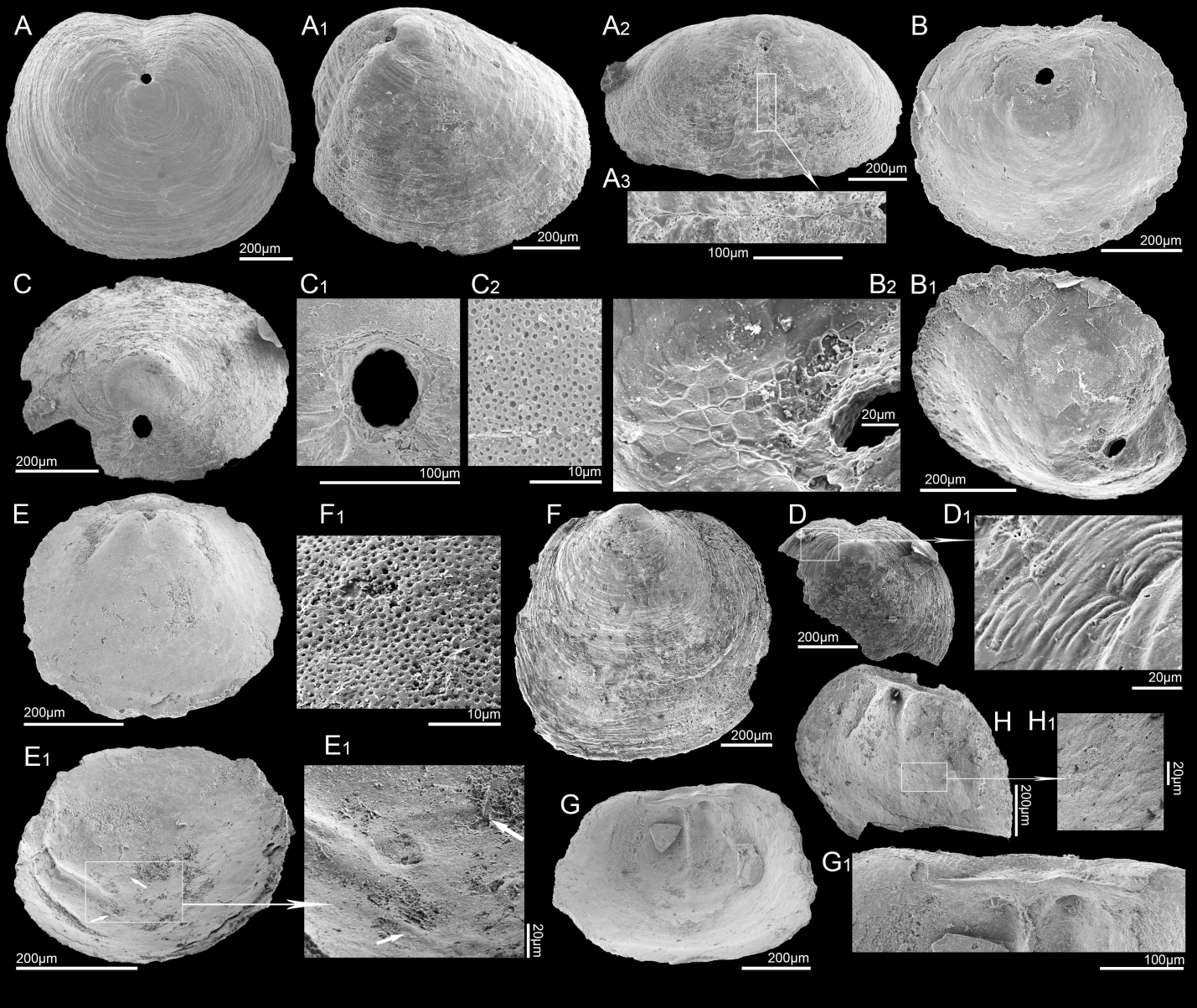
A
A1
A2
A3
B
B1
B2
C
C1
C2
D
D1
E
E1
F
F1
G
G1
H
H1
200μm
100μm
20μm
10μm

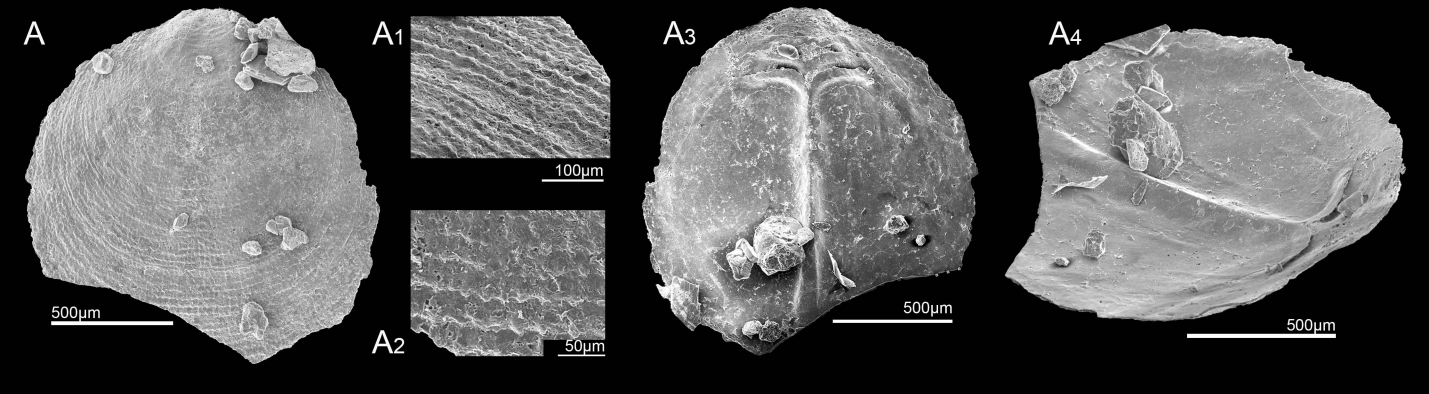
A
500μm
A1
100μm
A2
50μm
A3
500μm
A4
500μm

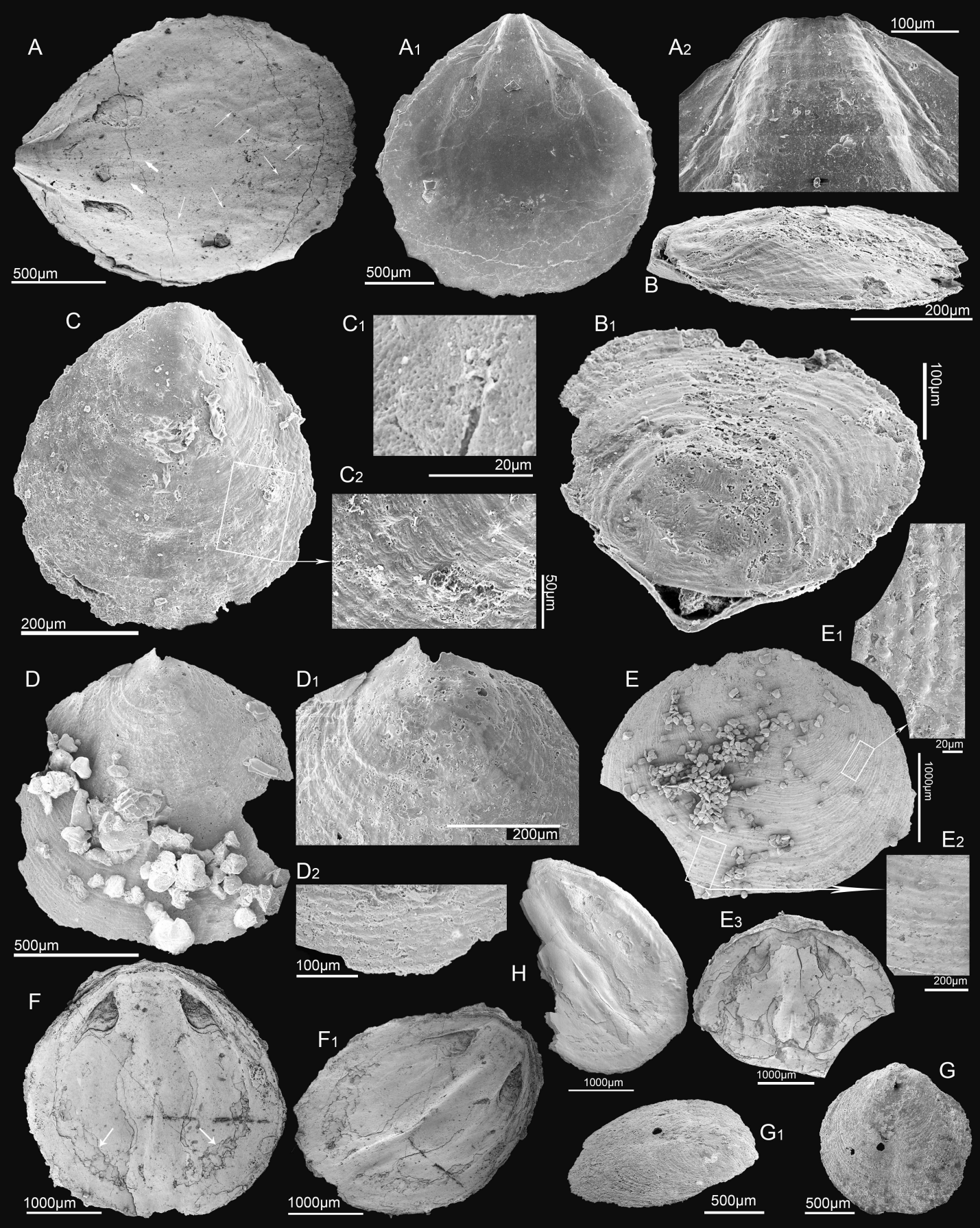
A
500μm
A1
500μm
A2
100μm
B
200μm
C
200μm
C1
20μm
C2
50μm
B1
100μm
D
500μm
D1
200μm
D2
100μm
E
E1
20μm
1000μm
E2
200μm
E3
1000μm
H
1000μm
F
1000μm
F1
1000μm
G1
500μm
G
500μm

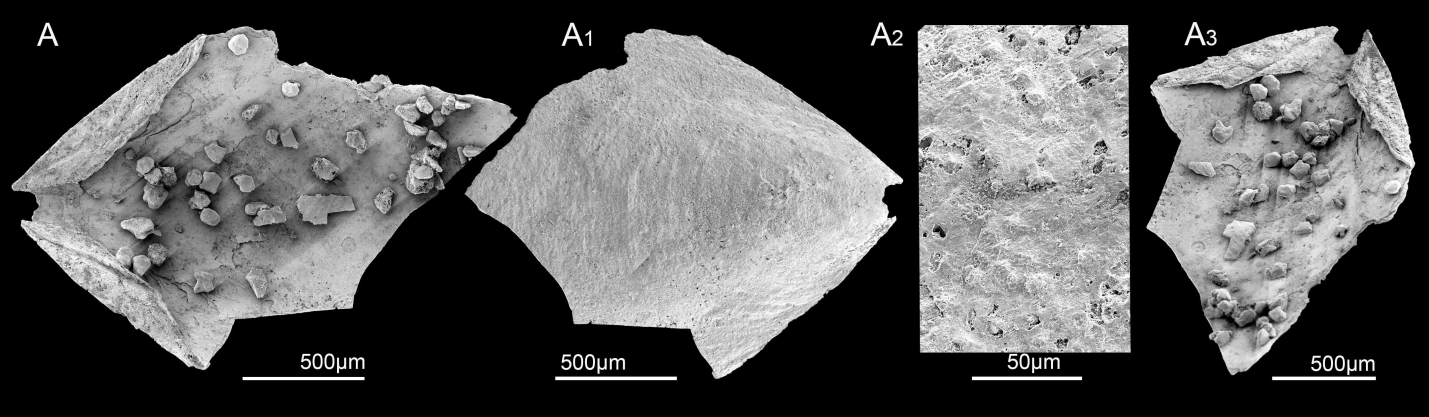
A
500μm
A1
500μm
A2
50μm
A3
500μm

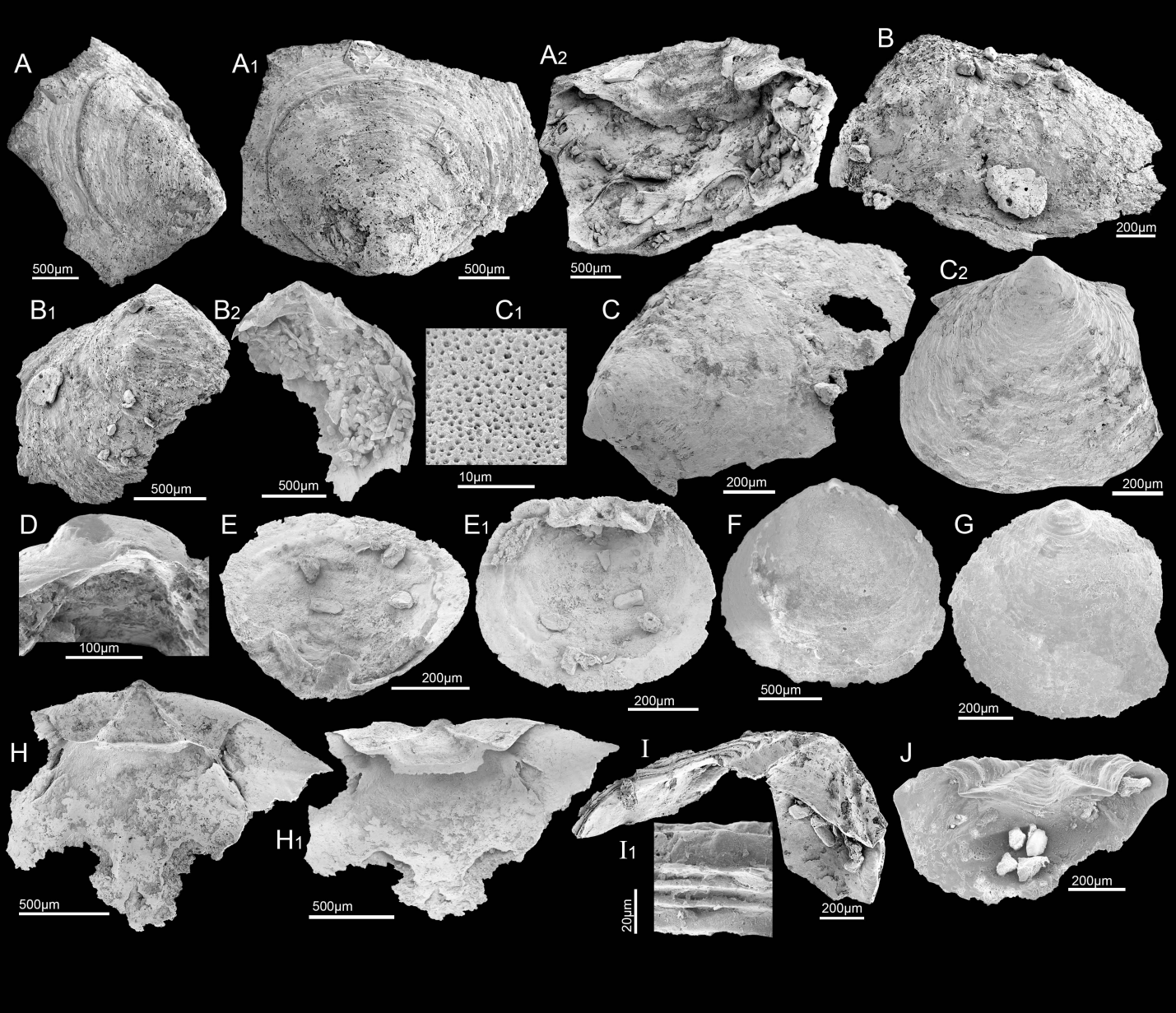
A
A1
A2
B
500μm
500μm
500μm
200μm
B1
B2
C1
C
C2
500μm
500μm
10μm
200μm
200μm
D
E
E1
F
G
100μm
200μm
200μm
500μm
200μm
H
H1
I
I1
J
500μm
500μm
20μm
200μm
200μm

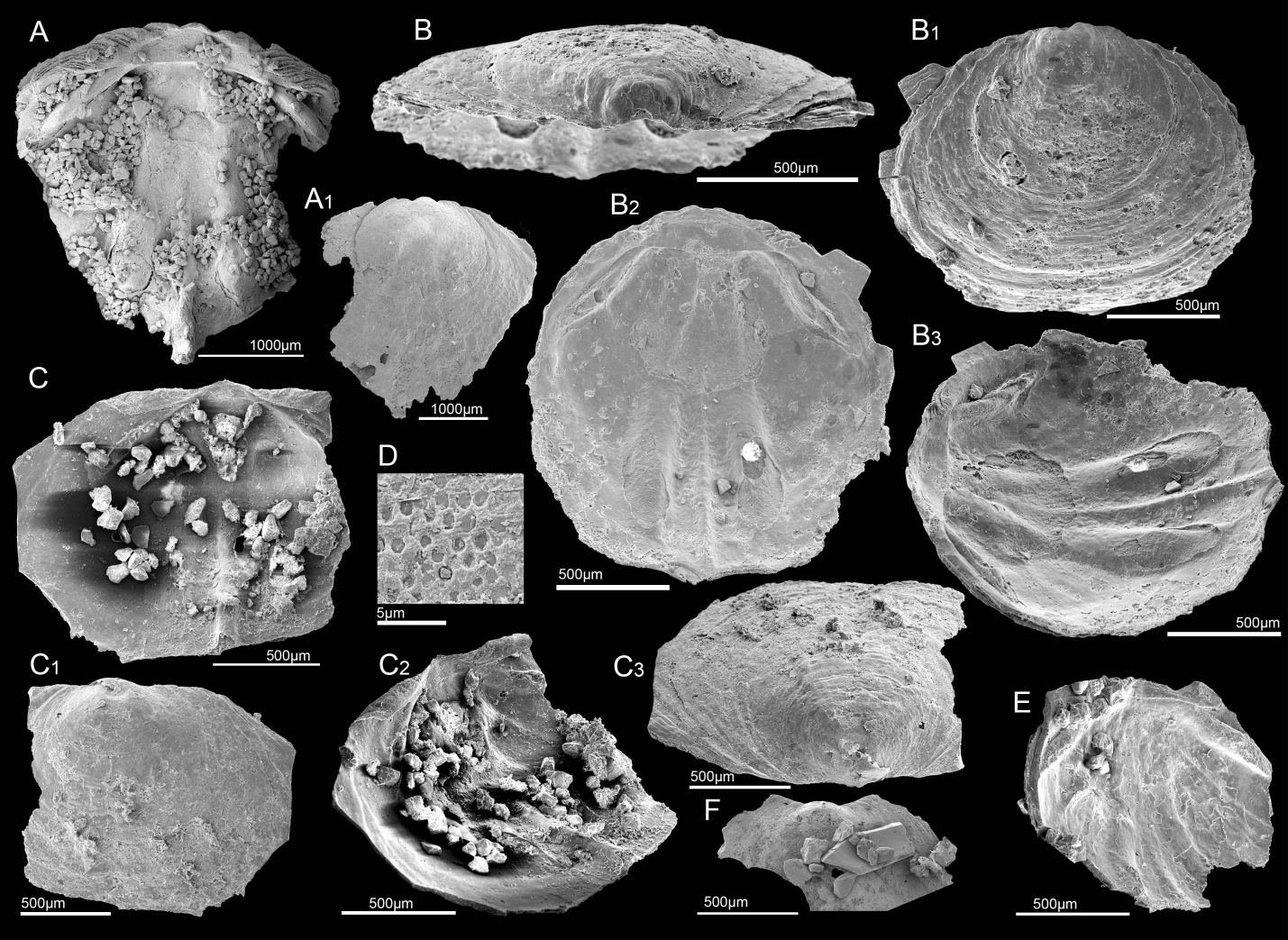
A
1000μm
B
500μm
B1
500μm
A1
1000μm
B2
500μm
B3
500μm
C
500μm
D
5μm
C1
500μm
C2
500μm
C3
500μm
F
500μm
E
500μm

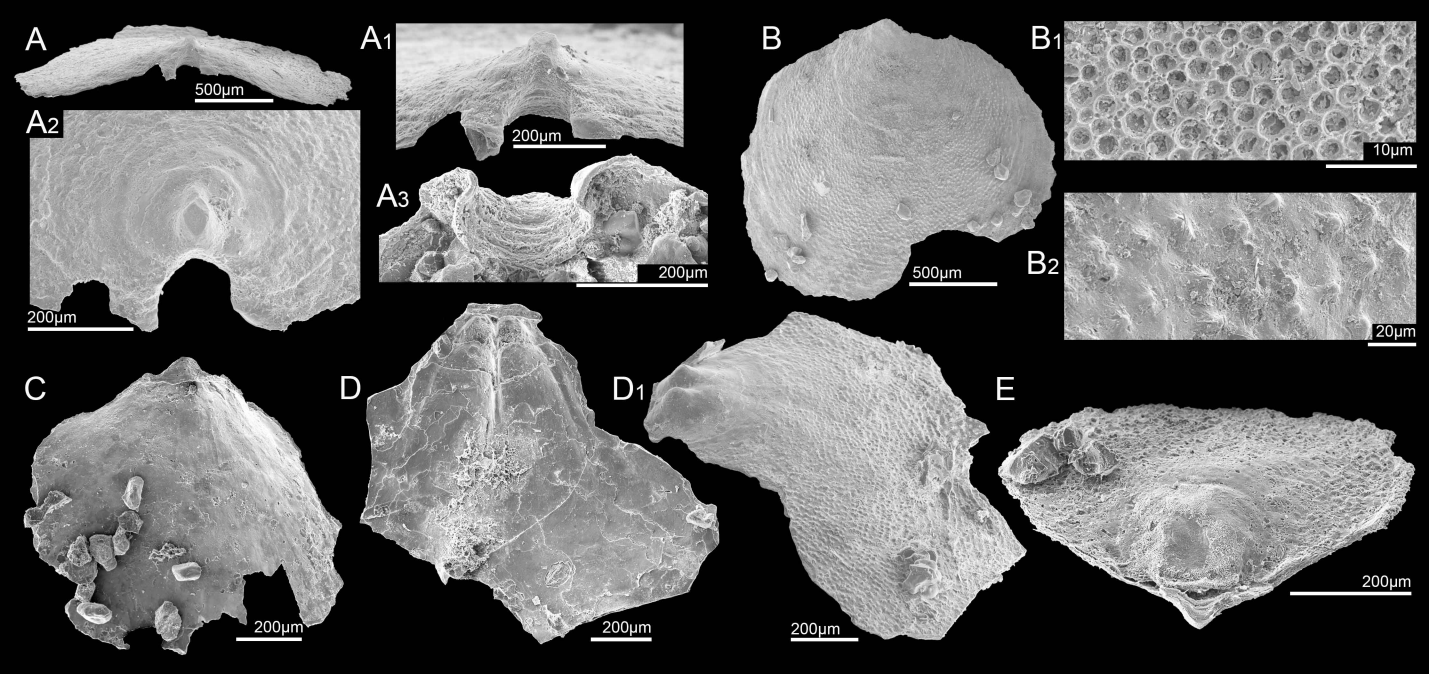
A
500μm
A1
200μm
A2
200μm
A3
200μm
B
500μm
B1
10μm
B2
20μm
C
200μm
D
200μm
D1
200μm
E
200μm